CHAPTER 1

INTRODUCTION

The chapter firstly discusses the background of the research in brief followed by the problem statement. After that, the objectives of the thesis, overview of the research methodology and the scope of the thesis are discussed sequentially.

1.1 Background

Brain tumor is a source of mortality and morbidity for which diagnosis and treatment require extensive resource allocation and sophisticated diagnostic and therapeutic technology. Global Burden of Diseases, Injuries, and Risk Factors (GBD) Study between 1990 and 2016 shows, the number of incident cases of brain cancer (which mainly lead from brain tumor) have increased across all geographical regions and SDI (Socio Demographic Index) quintiles, except for Eastern Europe where incident cases have remained stable. However, probably because of access to early detection and care, the mortality to incidence ratio decreases with improvements in SDI. For Bangladesh, there are 13 to 15 lakh cancer patients, with about 2 lakh patients newly diagnosed with cancer each year, where about 1.08 lakh people die each year. In this case, Head neck/ Brain tumors constitute about 2-5% cases. However, it is also one of the most curable forms of tumors if detected well on time. As such, scientists and researchers have been working towards developing sophisticated techniques and methods for identifying brain tumor. Although MRI and CT are the two modalities widely used for marking the abnormalities in terms of shape, size or location of brain tissues which in turn help in detecting the tumors, MRI is preferred more by the doctors. As a consequence, scientists and researchers have more focused on MRI. While identifying brain tumor from MRI images,

conventional inspection by physicians is mostly used. However, automated approaches mainly implemented by computer aided medical image processing technique are increasingly aiding physicians in detecting brain tumors. In this regard, medical image processing involves pre-processing (enhancement, filter application, segmentation, feature selection) and post-processing (identification and/ classification). These steps can be implemented by conventional machine learning approach as well as deep learning approach. In conventional machine learning approach, hand crafted features are used to obtain results from test image and the process is fast. In deep learning approach, models are tuned by appropriately selecting number of layers, activation function, pooling and sometimes pre-trained models are added for transfer learning. However, in both approaches metaheuristic algorithms may be used to enhance the classification accuracy. In broader perspective, this research will cover both conventional and deep learning approaches for identification of brain tumors from MRI images.

1.2 Problem Statement

A significant body of research has been conducted focusing to detection of brain tumours using MRI Images through machine learning approaches which recognizes the accuracies of a variety of emerging image processing techniques. Conventional machine learning approach is faster in comparison to deep learning. On the accuracy of deep learning approach is better than the conventional machine learning approach.

1.3 Thesis Objectives

The objectives of this research are, firstly, to explore how various image processing techniques are applied on MRI images for detection of brain tumor. Secondly, to compare the performance of existing image processing techniques applied on MRI images for

detection of brain tumor. Finally, to propose an efficient technique for detection of brain tumor using MRI images through machine learning approaches. As a result, this research will provide expected outcome ie efficient image processing technique to detect brain tumor using MRI images through machine learning approach which will assist pathology experts to provide proper treatment.

1.4 Methodology

The research has been carried out in three sequential phases. Firstly, research focusing on detection of brain tumors using MRI images was reviewed systematically. Secondly, drawbacks of existing techniques are identified from the literature. Basing on the deductions from phase I and II, efficient technique is suggested for detection of brain tumor from MRI images using both conventional and deep machine learning approaches. For conventional machine learning approach, few steps are followed. At first, MRI image data are collected from pathological experts where 3 different batches were incorporated. Image enhancement was then applied on to these images. For this case, at first grayscale images were converted in RGB images and then converted to HSV. After carrying out local histogram equalization, the images were converted back to RGB images. In second step, morphological operation is carried out on to these enhanced images. Then, segmentation is carried out which is the final step of pre-processing for the proposed framework. Here threshold based Otsu's segmentation was implemented on the image consisting of only green and blue channels while eliminating the red channel. For Post-processing, mainly 2 steps were used which include feature extraction and Identification of ROI (Region of Interest). Features can be categorized into 3 different categories which include shape, size and color features. This study incorporated pathology laboratory experts' used shape and size features which include regions area, circularity, solidity,

roundness, radius, and diameter. Prior to identification of the ROIs (obtained through the useful and necessary features), once again morphological operation was implemented as a fact that it assists binary segmented regions to have some shape and size reconstruction. Finally images of identified ROIs were placed over the original test image to check the results. The result was further validated using SVM classifier. For deep machine learning approach CNN is used. Here, the same data set is used as with the conventional machine learning approach. In this approach, the image set applied on a pre-trained model (vgg16). In the next stage, Conv2d (Convolutional layer) is applied setting filter size 32. Selecting filter size 40, 28, 16 did not show optimal results in CM (Confusion Matrix) and also in Train vs Validation Accuracy for each Epoch. In this architecture activation function was used. While applying ReLu as an activation function, it did not show optimal results but Sigmoid showed optimal results. In subsequent stage, Max Pooling is used. Here, 2x2 Max Pooling did not show optimal results but 4x4 showed optimal results. Here, 50% drop out is used. It was observed that increment in percentage of drop out increased number of nodes in the layers whereas decrement in in percentage of drop out increased computational intensity. Subsequently flatten layer was implemented. In the dense layer, use of Softmax as activation function did not show optimal results whereas application of Sigmoid as activation function showed optimal results.

1.5 Thesis Scope

The scope of this thesis has been limited to identification of brain tumors from MRI images only although there are other electronic modalities available for such identification like X-ray, CT Scan etc. The proposed framework for conventional machine learning approach, faster in processing, shows an accuracy of 96.23% which is well above the pathological threshold. It is likely to be suitable for pathologies with low

configured PCs which are commonly present in the laboratories of Bangladesh. On the other hand the proposed framework for deep machine learning approach which is computational intensive shows an accuracy of 97.84%. It is suitable for pathologies with high configured PCs.

1.6 Organization of the Thesis

The thesis is organized as follows:

Chapter 2 introduces the literature review focusing to the existing works. A critical summary is also presented to highlight the research gap and motivation to this research.

Chapter 3 provides the overview of the research methodology and briefly discusses the extensive empirical studies conducted in this thesis.

Chapter 4 highlights the experiment results for both the approaches.

Chapter 5 presents the main outcomes and contributions of this thesis followed by limitations and future work.

CHAPTER 2

LITERATURE REVIEW

This chapter provides a review of relevant literature related to this research. The objective of this study was to provide a conceptual information system framework for medical imaging using MRI brain tumor images in the histopathology laboratory. This was explored based on the related research works have been established to date. The role that microscopic manual analysis, electronic scanners and computer based approaches can play important role in histopathology image analysis are also examined. This review initially focuses on the application of available existing electronic scanners followed by computer based techniques and their application to improve the MRI brain tumor tissue analysis with a comparative accuracy in compare to manual analysis approach.

2.1 Medical Imagery

The review provides detailed information about the different types medical imaging analysis techniques in Section 2.2 which include microscopic image analysis, tissue analysis using electronic devices and computer based approaches. This is followed by a review of basic image processing techniques in Section 2.3 which includes data collection, pre-processing, segmentation and identification using feature information. Section 2.4 reviews research related image processing approaches to medical image processing domain which includes limitation or issues with medical imaging, clustering approach, feature selection and extraction, identification with classification. Section 2.4 reviews detailed information about medical image processing techniques. Section 2.5 reviews detailed information about ovarian tissue analysis techniques. The chapter

concludes in Section 2.6 with a summary of the findings of the review of literature including the gaps in knowledge that relate to the focus of this research.

This section considers all available methods that can be used for any types of tissue that can be analyzed in medical science. There are a number of possible ways which can be used to analyze tissues which include manual microscopic method, use of electronic devices and computer based image processing approaches.

2.1.1 Existing Available Approaches to Analyze Tissues

Routine examination of tissues is often necessary for diagnosis of various medical conditions. There are three possible ways to carry out this examination in the laboratory which include

i) Traditional microscopic analysis,

ii) Capturing the images using electronic devices (e.g. Ultrasound, CT, MRI, PET, X Ray) and analyse them,

iii) Computer based approaches using digitized images.

2.1.2 Traditional Microscopic Analysis

In the histopathology laboratory, experts examine slides of biopsy specimens using a microscope for counting and identification of numerous types of tissues. According to the domain expert information and from research study by (Lester, 2010) [1] indicates that typically sample tissues taken from a biopsy is sliced into thin segments (generally 5 – 20 microns), processed and placed onto glass slides. In addition to that preserving and staining is a part of processing the tissue segment in the preparation of histopathology slides. Generally pathology experts then carry out manual examination of these slides

using a microscope as a routine task at various magnification levels (e.g. 10x, 20x, 40x, 100x, 200, 400x) to make assessments. Typically, histopathology slides are more informative than other modalities as the process has the capability to preserve the tissue architecture (Gurcan et al., 2009) [2]. At present, analysis remains the "gold standard" (Kelsey, Caserta, Castillo, Wallace, & Gonzálvez, 2010) [3] for proof of presence of a diseased state and for changes in the distribution of specific cells across the tissue. While manual tissue analysis remains "gold standard", it has some limitations as it requires substantial amount of time for a single slide processing (typically 19-27 minutes for a single slide analysis using a microscope) by experts and experts have inter and intra observations variability issues (Van der Kwast et al., 2010) [4]. Additionally, instead of analyzing a huge number of biopsy slides for specific test (according to domain expert information generally 1000 – 2500 slides for a single test) experts randomly pick slides (Kothari, Phan, Stokes, & Wang, 2013) [5] (according to domain expert generally 100-150) and analyze them which in most cases do not provide accurate results.

With increases in computational power and the introduction of digital scanners and image processing techniques, digital histopathology image analysis allows experts to enhance to aid analysis the images. This reduces the time and effort required for diagnosis by pathologists as well as reduces human error and subjectivity (Lamprecht, Sabatini, & Carpenter, 2007) [6]. There are various types of digital scanners available at present to analyze various types of tissue structures which include Ultrasound, CT, MRI, PET.

2.1.3 Capturing the Images Using Electronic Devices (e.g. Ultrasound, CT, MRI, PET, X-Ray) and Analysis

There are various types of electronic scanners which are used in the histopathology laboratory for tissue analysis which include ultrasound, CT, MRI, PET, X-Ray are mostly used. Among all electronic scanning modalities ultrasound scanner is considered the most

popular due to the fact that it is cheap, portable and less risk to patients (Kiruthika & Ramya, 2014) [7]. Its limitation is that it can only process large and mature tissues (Skodras et al., 2009) [8]. In compare to Ultrasound the use of CT and MRI provide better when considering cancerous tissue specially brain tumors. Among CT and MRI images, MRI is considered more viable choice due to the fact that MRI images provide more information compared to CT images. However; expert intervention is essential to analyze these types of images.

2.1.4 Computer Based Approaches Using Digitized Images Acquired from the Slides of Biopsy Specimen

Manual microscopic analysis is time consuming, prone to errors and has inconsistent results among experts. Most used electronic scanner like ultrasound can only identify large and mature follicles. Additionally, CT, MRI and UT require experts' intervention. To overcome the issues associated with microscopic analysis and electronic scanners computer based approaches would be a viable choice as computerized image analysis reduces time, effort, human errors and subjectivity for the diagnosis of various tissues by pathologists (Lamprecht et al., 2007) [6]. There are various types of existing computer based approaches available at present which mostly considers cancer tissue analysis, blood vessel analysis and lymphatic vessel analysis. While there are so many existing approaches available to date hut none of the existing approaches are suitable to analyze MRI brain tumor tissues. This is due to the fact that none of the existing approaches are fully automated which do not require any human intervention when analyzing a new batch of images.

2.2 Image Processing Techniques

Computerized image analysis is a popular research area due to the fact that it is more reliable for its repeatable results and it reduces time, effort and human error. General image processing technique includes mainly three steps which include

a) Pre-processing

b) Segmentation

c) Identification and/classification

Pre-processing includes few steps which include correction of image intensity variations and elimination of noises. Each and every step includes various methods due to the fact that there are a number of ways to perform each step. From all existing related research works it is impossible to establish a universal approach as a fact that image processing is a broad research area.

2.2.1 Pre-processing

Pre-processing is performed as the first step of most existing semi-automatic and automatic image analysis techniques for MRI brain tumor image analysis. Pre-processing is aimed at:

a) Enhance contrast and

b) Noise removal.

2.2.1.1 Enhance Contrast

To reduce the illumination issues in the digitized images enhance contrast is a suitable option for image analysis which assists the following:

1) Better segmentation of MRI brain tumor images in the subsequent steps of semi-automatic and automatic algorithms.

2) Easier identification and/classification of cancer tissues.

However, there is no universal theory for enhance contrast approach (Nishu, 2012) [9]. Digitized images acquired from MRI are typically grayscale images. It is hard to deal with the intensity of a grayscale image straightway (Nishu, 2012) [9]. Grayscale images have various drawbacks such as only mature follicles can be identified.

For contrast enhancement histogram processing is one of the popular approaches. Histogram processing comprises with

1) Normalization (a method used to change the series of pixel intensity values based on relative frequencies) and

2) Equalization (a method that stretches the intensity range and improves the image contrast) approach.

Histogram equalization is widely used in medical image analysis for both semi-automated and automated approaches. Although histogram equalization approach is widely used technique in image analysis however; this approach often produces unrealistic effects (Entwistle, 2004, 2005) [10]-[11].

Some research work already has been done with MRI brain tumor images where histogram equalization approach was implemented.

2.2.1.2 Noise Removal Approach

It is important to remove unwanted regions as much as possible during pre-processing stage and therefore; all the existing approaches have used one of the noise removal techniques. For cancer cell detection median filter was used in the existing semi-automatic approach (Bapure, 2012 [12]; Liu et al. [13], 2004; Sertel et al., 2009 [2])

Kaur et al. (2020) [14] and in the existing automatic approach (Skodras et al., 2009) [8].

2.2.2 Segmentation

The second step of existing semi-automatic and automatic image analysis after pre-processing is segmentation to separate the regions likely to be cancer tissues from other tissues. The purpose of segmentation is to partition a digital image into meaningful or perceptually similar regions. Existing work in the literature has applied different methods such as edge based approaches (Picut et al., 2008) [15] ,threshold based approaches(Kelsey et al. [3], 2010; Landini & Othman [16], 2003; Liu et al., 2004 [17]; Picut et al., 2008 [15]; Sertel et al., 2009 [2]; Skodras et al., 2009 [8])and by using mathematical morphology (such as the watershed approach(Bapure, 2012 [12]; Landini & Othman, 2003 [16]; Skodras et al., 2009 [8])).

From the literature review most researchers have used threshold operator (different threshold value with different threshold operator to fit get the segmented image) to segment the ROIs from other regions Goh et al. (2018) [18]. Hysteresis threshold operator refers to as segmentation of regions from background using both lower and upper value whereas a standard mode of thresholding uses only lower value to perform the threshold. Moreover, Skodras et al. (2009) [8] have used morphological closing operation using dilation operator to dilate their images to remove unwanted regions which are less than the lower threshold value and upper than the higher threshold value. These two values have helped them to reduce much unwanted regions for their test images. Cluster based segmentation named K-means Telrandhe et al. (2016) [19], Ahmmed et al. (2016) [20], Wu et al. (2007) [21] and C-means clustering approaches were also incorporated.

It is noticeable that Landini and Othman (2003) [16] have used threshold operator before using the noise removal algorithm because they have used a different approach to achieve

a better result after automatic segmentation. Liu et al. (2004) [13] have implemented Object density based segmentation approach for their proposed semi-automatic approach.

2.2.3 Identification and/Classification

The third and final step of existing semi-automatic and automatic image analysis approach is to detect the follicles based on follicle characteristics. For MRI brain tumor images there are three basic characteristics (shape, size and colour) required. Size is used to put a pixel boundary (minimum and maximum pixel value) to keep the required ROI. Shape is used to find the follicles having the desired shape rather than unwanted ones. Sometimes size based approach cannot full-fill to detect the required ROI and thus circularity parameter is used (minimum and maximum circularity) to put a boundary for the circularity shape.

Thaha et al. [22] proposed a deep learning method using CNN for the segmentation. This method employs 3x3 small kernels for the deep architecture of CNN model. Intensity normalization and data augmentation have been performed for the preprocessing of images. Kebir et al. [23] proposed a supervised method for detecting the brain abnormalities form the MRI images in three steps, first step is to develop a deep learning CNN model, then subdivision of brain MRI images is done by the k-mean algorithm followed by brain component classification as normal or abnormal classes according the developed CNN model. Vinoth et al. [24] proposed a programmed division strategy based on CNN. Here, kernels are used for the purpose of classification and SVM classification is performed with the calculated parameters. And, extraction and detection of tumour from MRI scan images of the brain is done by using MATLAB tool. A three Incremental Deep Convolutional Neural Network 2CNet, 3CNet and EnsembleNet for automatic brain

tumor segmentation has been proposed in [25]. This method adopted the technique of Ensemble Learning and to avoid the hit and trial for training the CNN, they bounded the hyper-parameters to accelerate the training.Mohsen et al. [26] used DNN for classifying a dataset of 66 brain MRIs into 4 classes (normal, glioblastoma, sarcoma and metastatic bronchogenic carcinoma tumors). Classifier was combined with the DWT and PCA. An automatic brain tumor segmentation algorithm [27] has been proposed using Deep Convolutional Neural Network. They have used 2phase training procedure and explored cascade architecture to use basic CNN output as an additional information source.An effective brain tumor segmentation form MR images has been proposed in [28] by extracting the relevant features form combining the segmented pathological tissues, white matter, gray matter and fluid (CSF) and then classifying them using the Neural Network model. The comparison has been done by implementing the k-nearest neighbor classifier and Bayesian Classifier.

2.3 Discussion

Nishu (2012) [9] mentioned that there is no universal theory for image enhancement but rather based on test images a suitable technique can be implemented. Moreover, some researchers have not used any enhancement approach at all(Kelsey et al., 2010) [3]. In these circumstances, for this research study depending on the image characteristics it is important to examine whether to enhance the image contrast is necessary or not.

There are different noise removal algorithms available. Some existing approaches have implemented median filter, mean filter and /or average filter for their proposed method during pre-processing. However, it is not mandatory that noise reduction algorithm should be implemented at the pre-processing stage as Landini and Othman (2003) [16] have used noise removal algorithm after segmentation. Again, for this research study it is

important to examine which noise removal algorithm should be used, how many times and in which step it will be implemented.

Only a few researchers have used edge based approach during segmentation(Picut et al., 2008) [15] . However, threshold based segmentation was implemented for almost all the approaches (Kelsey et al. [3] , 2010; Landini & Othman, 2003 [16] ; Liu et al. [13], 2004; Picut et al., 2008 [15]; Sertel et al., 2009 [2] ; Skodras et al., 2009 [8])including mathematical morphology (such as the watershed approach(Bapure, 2012 [2]; Landini & Othman, 2003 [16] ; Skodras et al., 2009 [8])). There are more than 10 different threshold algorithms available. For this research MRI brain tumor images it is necessary to explore the best fit threshold algorithm which will help this research work to identify the cancer tissue while considering the shape and size attributes.

To identify the regions during follicle detection researchers have implemented shape, size and colour based approach but for most of the approaches have not used all the parameters (shape, size and colour). However, the result needs to be validated by a histopathology expert no matter it is a semi-automatic or an automatic approach and therefore, this research study needs to explore the best features from the segmented regions.

Ser	Existing Work	Steps Used	Identification
1.	Kaur et al. (2020) [14]	• Modified median filter and multi-vector segmentation machine is used to form the segmented tumor region in the images. • Implementation of the suggested techniques is evaluated with multi support vector algorithm which distinguishes the tumor and MRI images.	Brain Tumor
2.	Pandiselvi et al. (2019) [29]	• Proposed a novel method called Adaptive Convex Region Contour (ACRC) algorithm • SVM is utilized for slice classification whether it is normal or abnormal • After obtaining SVM results, abnormal slices are involved in segmentation process	Brain Tumor

3.	Tiwari et al. (2020) [30]	• Study compares two most trending techniques- conventional machine learning techniques and deep learning applied with metaheuristic algorithms.	Comparison of techniques
4.	Wahlang et al. (2019) [31]	• Compares various segmentation techniques for Brain Tumor from MRI	Comparison of techniques
5.	Goh et al. (2018) [18]	• Analyzes the performance of image thresholding for otsu • Found that success of image segmentation depends on object-background intensity difference, object size and noise measurement • Also found that it is unaffected by location of the object on that image.	Performance of otsu
6.	Telrandhe et al. (2016) [19]	• Used k-Means segmentation with preprocessing of image • object labeling used for more detailed information of tumor region • To make the system an adaptive one, used SVM • Implemented in supervised manner	Brain Tumor
7.	Ahmed et al. (2016) [20]	• Proposed Template based K-means and Modified Fuzzy C-means (TKFCM) • K-means algorithm emphasized initial segmentation through the proper selection of template • Updated membership is obtained through distances from cluster centroid to cluster data points, until it reaches to its best. • on the basis of updated membership and automatic cluster selection, a sharp segmented image is obtained with red marked tumor from modified FCM technique	Brain Tumor
8.	Amare et al. (2018) [32]	• an automatic brain tumor detection and segmentation framework has been proposed	Brain Tumor
9.	Logeswari et al. (2010) [33]	• Proposed use of Hierarchical Self-organizing Map (HSOM) which is an extension to SOM (2010)	Brain Tumor
10.	Wu et al. (2007) [21]	• Proposed K-means clustering basing on the idea that number of clusters is usually known for images of particular region of the human anatomy	Brain Tumor

Table 2.1: Medical image analysis on MRI brain tumor images (Conventional ML)

The table (2.1) indicates that related works are based conventional image analysis approach which includes enhancement, filter, segmentation and identification and/or classification.

Ser	Existing Work	Steps Used	Identification
1.	Chanu et al. (2020) [34]	• Proposed 2D CNN classification technique • Classified MR images into two classes (normal and tumor) • Accuracy with 97%, sensitivity with 100% and Specificity with 94%.	Brain Tumor
2.	Shibly et al. (2020) [35]	• Proposed DNN based Faster Regions with CNN (Faster R-CNN) framework was proposed • Detect COVID-19 patients from chest X-Ray images using available open-source dataset • Classification accuracy of 97.36%, sensitivity 97.65%, precision 99.28%	COVID-19
3.	Thaha et al. (2019) [22]	• Proposed a deep learning method using CNN for the segmentation. • Method employs 3x3 small kernels for the deep architecture of CNN model • Intensity normalization and data augmentation have been performed for the preprocessing of images	Brain Tumor
4.	Kebir et al. (2018) [23]	• Proposed a supervised method for detecting the brain abnormalities form the MRI images • Developed a deep learning CNN mode • Subdivision of brain MRI images is done by the k-mean algorithm • Classification of brain component as normal or abnormal classes according the developed CNN model.	Brain Tumor
5.	Vinoth et al. (2018) [24]	• Proposed a programmed division strategy based on CNN • Kernels are used for the purpose of classification • SVM classification is performed with the calculated parameters • Extraction and detection of tumor from MRI scan images of the brain is done by using MATLAB tool	Brain Tumor

6.	Ben et al. (2018) [25]	• Proposed a three Incremental Deep Convolutional Neural Network 2CNet, 3CNet and EnsembleNet for automatic brain tumor segmentation • This method adopted the technique of Ensemble Learning • Bounded the hyper-parameters to accelerate the training in order to avoid the hit and trial for training the CNN	Brain Tumor
7.	Mohsen et al. (2018) [26]	• DNN was used for classifying a dataset of 66 brain MRIs into 4 classes (normal, glioblastoma, sarcoma and metastatic bronchogenic carcinoma tumors) • Classifier was combined with the DWT and PCA	Brain Tumor
8.	Havaei et al. (2017) [27]	• Proposed an automatic brain tumor segmentation algorithm using Deep CNN • Used 2phase training procedure and explored cascade architecture to use basic CNN output as an additional information source	Brain Tumor
9.	Damodharan et al. (2015) [28]	• Proposed an effective brain tumor segmentation form MR images • Extracted the relevant features form combining the segmented pathological tissues, white matter, gray matter and fluid (CSF) • Classified them using the NN model • The comparison has been done by implementing the k-nearest neighbor classifier and Bayesian Classifier	Brain Tumor

Table 2.2: Medical image analysis on MRI brain tumor images (Deep ML)

The table (2.2) indicates that related works are based machine learning based image analysis approach which include various types of classification approaches for identification and/o classification basing on Deep ML.

Ser	Existing Work	Findings
1.	Tiwari et al. (2020) [30]	• Methods mostly used are: ❖ Standard machine learning techniques - SVM, SOM ❖ Deep learning based techniques- CNN, DCNN, G-CNN ❖ Metaheuristic algorithms- GA, DE, PSO, Bat algorithm, ABC ❖ Data mining tools- FCM ❖ Hybridization techniques
2.	Kumari et al. (2018) [36]	• For clustering algorithm mostly used ❖ Particle swarm optimization (PSO), fuzzy c-means and k-means • The selection of algorithm is done to achieve maximum accuracy in minimum time • But, for classification SVM has been used by most of the researchers
3.	Wainer et al. (2016) [37]	• Comparing 14 very different classification algorithms (random forest, gradient boosting machines, SVM - linear, polynomial, and RBF - 1-hidden-layer neural nets, extreme learning machines, k-nearest neighbors and a bagging of knn, naive Bayes, learning vector quantization, elastic net logistic regression, sparse linear discriminant analysis, and a boosting of linear classifiers) on 115 real life binary datasets, it was found that highest accuracy shown by: ❖ SVM ❖ Random forest ❖ Gradient boosting ❖ Naïve Bayes
4.	Tiwari et al. 2020 [30]	• Among all the used techniques, commonly used ones are: ❖ CNN (14%) and PSO (*Particle Swarm Optimization*) (14%) ❖ SVM (10%) and FCM (10%)

Table 2.3: Important Literature findings

2.4 Summary

1) None of the existing approaches are fully automated as calibration of processing parameter is essential.

2) If one batch of image works with one specific parameter new batch of images requires modification of parameters again.

3) None of the existing approaches have validated their proposed approach with other existing approaches.

4) Accuracy rate does not meet the “gold standard” criteria.

5) Human intervention is essential.

CHAPTER 3

METHODOLOGY

This chapter firstly provides the overview of the research methodology. Then onwards, it briefly discusses the extensive empirical studies conducted in this thesis.

3.1 Introduction

This chapter focused and outlines the materials (dataset) and methods used in this research study. The chapter describes the research methodology, research approach and research activities of this study. This is followed by the description of the datasets and source from where the dataset were collected. The rest of the chapter details the data preparation and preprocessing methods, data analysis techniques, and validation techniques. The chapter concludes with the details of the software platform and a chapter summary.

3.2 Research Methodology

There are a numerous types of research works available to date which can be categorized as diagnostic research, qualitative research and quantitative research (Kothari, 2004) [5]. All these types of research works do not follow the same research methodology. The research methodology used in this study includes a combination of diagnostic research and quantitative approach. This research study also considered quantitative based approach.

3.3 Research Approach

The research approach for this study used multiple phases as shown in Figure 3-1. These phases included the identification of research problem, literature review, formulating research

methodology, identifying the gaps and issues from existing approaches, collection of data, data analysis, and validation of proposed approach.

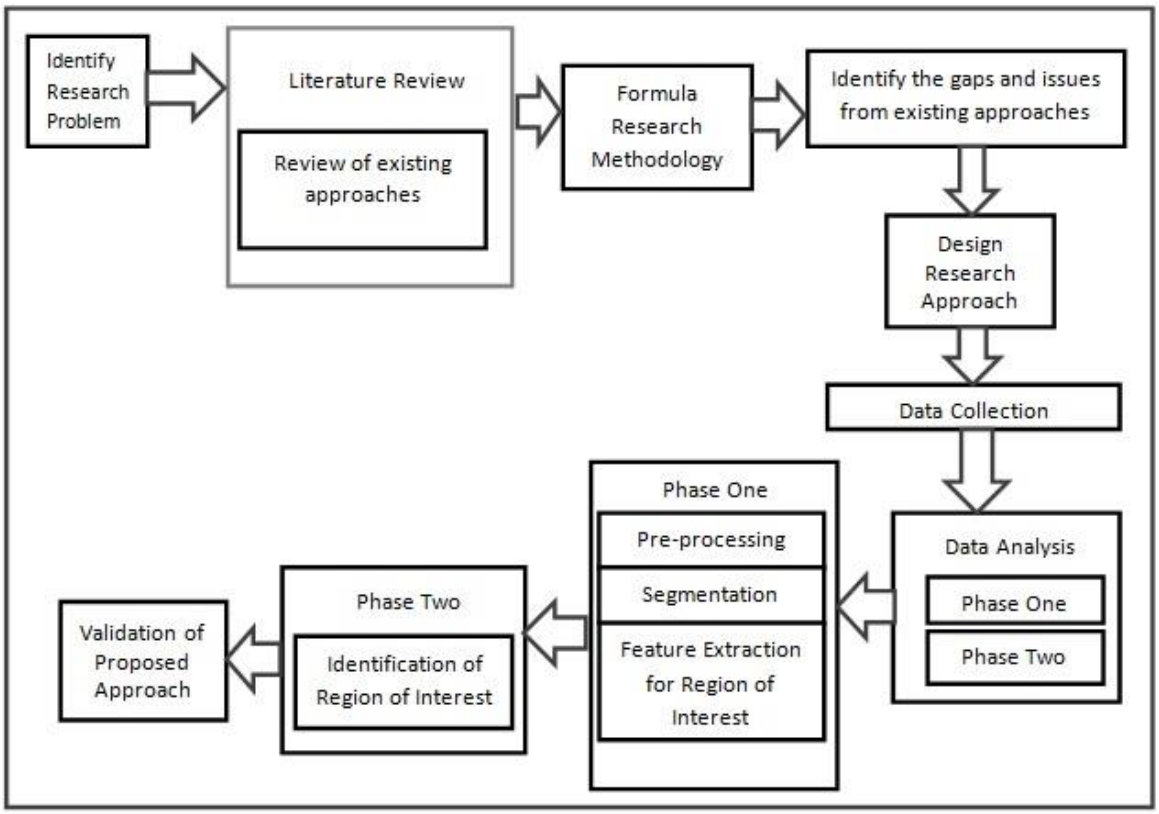

Figure: 3-1 Research Approach

3.4 Research Activity

3.4.1 Data Collection

The datasets were collected from Talukder Pathology, Mymensingh, Bangladesh. Additionally, one of the medical experts' Mr. Md. Sadequel Islam from the same pathology laboratory was nominated as the domain expert for this research study. Nominated domain expert is a renowned histopathology expert and was as an Associate Professor in Dinajpur Medical College, Bangladesh.

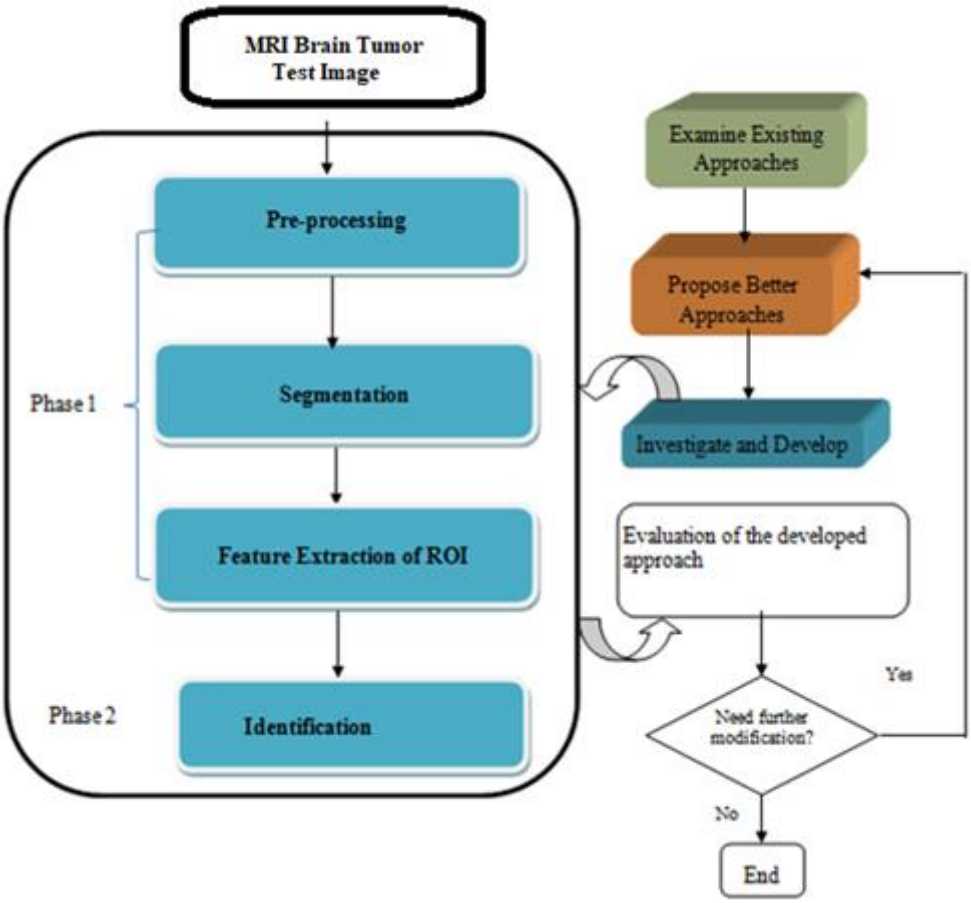

Figure 3-2: Research activity plan (on the right), with steps for the proposed approach (on the left).

3.4.2 Development of Proposed Approach

Using the research activity plan shown in Figure 3-2 this study has incorporated two research activities and among them activity two provides the most accurate results in compare to the results obtained using conventional image processing approach. Detailed description of this study proposed approach is available in chapter 5.

3.4.3 Dataset Used in this Study

This study considered a total of 502 brain tumor images acquired from MRI. All the images are in JPEG format (32 bits) and the test image size is 500 x 500. Detailed information is shown in Table 3-1.

Image Batch	Number of Annotated image	Number of Non-annotated image
Batch One	167	167
Batch Two	178	178
Batch Three	157	157

Table 3-1: Composition of research test image dataset

3.4.4 Validation of the Proposed Approach

Working with medical image datasets is always challenging for a non-medical expert. Medical experts know which cell belongs to which group (i.e. blood vessels, lymphatic vessels, cancer tissues, and reproductive tissues). Additionally, they can validate the results accurately. For a non-medical expert or more specifically for a non-medical background image processing experts, it is necessary to get assistance from medical experts to analyze tissues accurately. This assistance can be categorized in two different ways which include

i) To validate the test results from medical experts' immediately after the processing and/or

ii) To obtain two different image datasets that are identical to each other (one test dataset and the other one is the marked regions from experts for the same datasets) and then validate the test results with the marked regions.

Figure 3-3 is a sample of a corresponding pair of marked and unmarked images but identical to each (3 different magnification but for same regions) other used as test data in this research study.

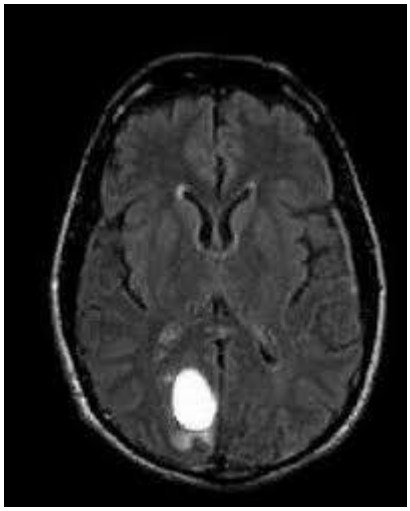

(a) MRI Brain Tumour Image (research test image)

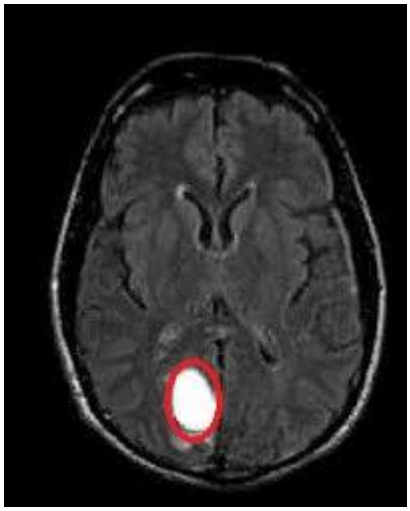

(b) MRI Brain Tumour Image (marked by experts)

Figure 3-3: an example of expert marked (b) and test (a) images which are identical to each other collected from the medical laboratory and used in this research study.

Data	Experts marked images	Test images
Training data set	A	A
Unseen Test data Set	B	B

Table 3-2: Partition of the full datasets into training dataset and unseen test dataset

Table 3-2 indicates that the image dataset used in this research study will be randomly grouped into a training dataset (consisting of a number of test images with their corresponding experts marked images). This randomly selected test dataset will be used in the development of the proposed technique and unseen test dataset will be used to evaluate the performance of the developed techniques. Validation will be carried out while comparing the results of this study proposed approach and experts' marked regions in an image.

3.5 Techniques

This research study has followed the Research methodology plan (Figure 3-2) where there are two phases mentioned. In the literature review it has been mentioned that in each of the phases more than 1 step can be incorporated for image processing. For each and every step there a various types of algorithms are available at present. First priority is to keep the image processing as simple as possible for which basic image processing steps should be used to see of that works well for a specific dataset or not. The second priority is to test and try different existing algorithms to see which algorithm is suitable for a specific set of images. If exiting approaches do not provide satisfactory outcome then it is necessary to propose a new approach or at-least a modified approach to attain satisfactory results. Final and third priority is to compare the computerized results with the human analysed results for validation and accuracy.

Based on the literature review this research study incorporated most related and most used techniques. Finally, this research study modified or proposed a new technique where necessary for each step and proposed a suitable and accurately workable approach for this research study test image datasets.

3.5.1 Pre-processing

For a computerized image processing perspective pre-processing is considered as the initial step of phase 1. Pre-processing step may have one or more steps which include

i) Intensity enhancement and / or

ii) Elimination of unwanted regions or noise elimination approach.

3.5.1.1 Intensity Enhancement

It is not always mandatory to use both pre-processing steps for each and every image processing techniques but depending on the dataset, issues associated with the dataset one or both options can be incorporated for analysis and identification purposes.

Images that are acquired from the histopathology laboratory may or may not have intensity dissimilarity around the image. If the dataset if free from intensity dissimilarity issues then it is not necessary to use the step (i) image intensity enhancement but rather (ii) Elimination of unwanted regions or noise elimination approach would be a viable choice to use as the first step for pre-processing.

3.5.1.2 Elimination of Unwanted Regions for Image Analysis

During image acquisition using electronic scanners unwanted noise may occur due to poor signals from scanners. It is important to remove this type of unwanted regions acquired from electronic scanners especially from MRI. This type of removal application can be referred to as noise reduction or filter approach.

At present there are several types of filter approaches available to eliminate noises. For medical image analysis especially for cell analysis perspective (i.e. cancer, ovarian reproductive cells) commonly used filters are Mean and Median filters (Bapure, 2012 [12]; Liu et al., 2004 [13]; Sertel et al., 2009 [2]; Skodras et al., 2009 [8]).

3.5.1.2.1 Mean Filter

Mean filter is a simple type of filter which has the capability to reduce the intensity variation between two pixels close to each other for which mean filter is a viable choice for smoothing operation. The main idea of a mean filter is it replaces each pixel value using the average value from a given window in an image. Additionally, using a mean

filter with a given windows size it is also possible to remove unrepresentative surrounding the pixel values. The formula for mean or average filter simple as a fact that sum up elements and divide the sum by the number of elements will give the average value.

This type of filter can be generally referred to as a convolution filter as a fact that like other convolution filters it also works using a window size or a kernel. This kernel is used to perform the mean calculation of the neighborhood. An example of mostly used kernel for mean filter is 3 x 3 square kernel. Smaller sized kernel is used when less smoothing performance is required and larger kernel is used when extensive smoothing operation is required.

There are two major issues in mean filter operation which include

- Any single pixel inside the selected window which does not have any representative value can notably change the mean value of all the pixels for all the neighborhood pixels.
- An edge that is overlapped by the filter neighborhood generally interpolates new pixel values on the edge and consequently the edge becomes blurry. For a sharp edge filter operation this is a notable drawback for mean filter.

3.5.1.2.2 Median Filter

In compare to a mean filter, median filter is a well-known approach for image processing as a fact that median filter is referred to as a nonlinear digital filter to eliminate noises. Additionally, it has better capability to preserve image edges in compare to a mean filter. However, one of the major drawbacks is, median filter also has blurry effect and requires longer processing time. Selection of an appropriate cut-off radius along with a proper

mask size would be useful to minimize blurriness but for ovarian tissue (differs in shape and size) analysis it is a hard task to select a suitable cut-off radius.

3.5.1.2.3 Filter using Mathematical Morphological Operation

Unwanted regions can also be eliminated using mathematical morphological operations which include erosion, dilation, morphological opening, morphological closing, bottom hat and top hat filters.

3.5.2 Segmentation

After a successful pre-processing stage the next step is to segment the regions of interest in such a way that it helps to perform an efficient identification. Currently, there are a numerous number of segmentation approaches available which include grayscale and color image segmentation approaches. Images acquired from electronic scanners are manly grayscale images and hence grayscale image segmentation is always a viable option. Among all available grayscale segmentation approaches threshold based segmentation is the most popular one.

3.5.2.1 Threshold Based Segmentation

Thresholding is referred to as a most simple technique for image segmentation. From a grayscale image; thresholding technique is used to create a binary image. This is a simple but an effective technique to partition or segment an image into background and foreground. For image processing perspective, regions of an image correspond to objects that are useful for analysis is partitioned correspond to background. Using this approach segmentation mainly carried out while isolating the objects by switching gray-scale images to binary images. More often this approach provides an easy way to perform

partitioning based on the intensity difference among foreground and background of an image. This is due to the fact that this approach uses a specified range of intensity for partitioning. As for example, if the range is set up 127 then anything that has a greater value than 127 in the grayscale image can be set to 1and anything below127 can be set to 0 in the binary image. This process can be referred to as fixed thresholding as a fact that the threshold values is set to 127.

For segmentation approach the input images can be either a grayscale of a color image and for the simplest implementation the output is a binary image. Binary images are black and white image where pixels with black color correspond to background and white pixels correspond to foreground and vice-versa. To perform this operation for the simplest operation a single parameter is used referred to as intensity threshold. For a single pass application each pixels in the images is compared with the intensity threshold value. Higher pixel intensity values in compare to intensity threshold value will become white and lower pixel intensity values will become black.

It is also possible to use multiple intensity threshold values as for example a band of intensity values can be set to white and the intensity values which do not fall in between the band intensity value range will become black and vice-versa. Another option can be used which include to set black all the pixels those corresponds to background while leaving the foreground unchanged.

For an automated segmentation approach using threshold based approach it is necessary to select the threshold value automatically rather than a manual random selection.

Otsu's threshold based segmentation approach follows clustering based approach. Similar to general threshold approach this approach also uses two classes (foreground and background) while following the bi-modal histogram (foreground and background pixels) and then computes the threshold value.

Otsu's method may not work in presence of noise as a fact that smoothing operation before segmentation will not even help to minimize the loss of information using Otsu's method.

OTSU threshold based segmentation approach was incorporated by (Kelsey et al., 2010 [3]; Landini & Othman, 2003 [16]).

3.5.2.2 Clustering Approach

There are a number of clustering techniques available for the identification process. Most approaches require a pre-defined cluster parameter to perform clustering operation and among all available clustering approaches k-means is considered as the most common one.

3.5.2.2.1 K-means Clustering Approach

Based on the operational perspective clustering can be defined as an existing representation of n items estimate the number of groups using on the pre-dined group number (K) based on the similarity measure criteria (group items in a same group with high similarity and lastly items with less similarity in another group). A good cluster is a set of compact and isolated points. It is always a challenge to group items with an unknown number of clusters as a fact that for a given data points there are numerous number of existing clustering algorithm using unknown number of clusters and it is hard to use a suitable one from them.

In computer vision one of the important issues is segmentation approach which can also be designed as a clustering problem.

Data clustering is generally used for the following three main purposes.

(1) To know the underlying structure: to detect irregularities and identify most relevant features.

(2) Natural classification: to classify the similarity between items available in a given set of data.

(3) Compression: To organize the data using a suitable cluster prototype.

Depending on what types of data need to be analyzed clustering can also be named as Q-analysis, typology, clumping and taxonomy.

3.5.2.2.2 Feature Extraction

Feature selection, is a problem closely related to dimension reduction. The objective of feature selection is to identify features in the data-set as important, and discard any other feature as irrelevant and redundant information. Since feature selection reduces the dimensionality of the data, it holds out the possibility of more effective & rapid operation of data mining algorithm (i.e. Data Mining algorithms can be operated faster and more effectively by using feature selection).

Conventional supervised FS methods evaluate various feature subsets using an evaluation function or metric to select only those features which are related to the decision classes of the data under consideration. However, for many data mining applications, decision class labels are often unknown or incomplete, thus indicating the significance of unsupervised feature selection. In unsupervised learning, decision class labels are not provided.

Principal Components Analysis (PCA) is the predominant linear dimensionality reduction technique, and it has been widely applied on datasets in all scientific domains. In words, PCA seeks to map or embed data points from a high dimensional space to a low dimensional space while keeping all the relevant linear structure intact. To improve the efficiency and accuracy of data mining task on high dimensional data, the data must be preprocessed by an efficient dimensionality reduction method. Principal Component Analysis (PCA) is a popular linear feature extractor used for unsupervised feature

selection based on eigenvectors analysis to identify critical original features for principal component. PCA is a statistical technique for determining key variables in a high dimensional data set that explain the differences in the observations and can be used to simplify the analysis and visualization of high dimensional data set, without much loss of information. Rough set theory is employed to generate reducts, which represent the minimal sets of non-redundant features capable of discerning between all objects, in a multi objective framework. Rough-PCA approach is the combination of PCA and Rough set theory.

3.5.3 Identification and/ Classification

3.5.3.1 Identification

Generally the final step of image processing is identification step unless classification approach is involved to increase the accuracy rate. Due to different shape, size and colour variation it is necessary to consider features such as shape, size and color based features during identification. There are many features which can be used to identify the regions including both object level features and spatial arrangement features but all features are not essential for reproductive tissue identification (T. Sazzad et al., 2015) [38]. The selection of too many redundant features can be problematic as it may result in an ineffectiveness of main features for identification. The term feature selection (FS) is a procedure for selecting more informative features. Feature selection approach can limit this problem and improve identification. It can also assist in the efficient selection of minimum number of features from a large number of original feature set.

Research by stated that there are two ways to select necessary features from a large number of feature set. The first approach is referred to as the feature extraction approach

where original feature space is considered and then most effective features using of all the data are mapped to a lower-dimensional subspace. The same study mentioned that the main purpose of using feature extraction is to eliminate unnecessary information from the feature set. There are many feature extraction approaches available including principal component transform analysis (PCA), projection pursuit and feature removal based on separability criteria are most common which are already described in the earlier section. The second approach is referred to as feature choice or band choice where a small subset of features is responsible for class representation. Common feature selection methods include PCA-based band selection, information-entropy-based band selection and class-separability-based band selection. This research study considered different types feature selection approaches to identify the regions of interest.

3.5.3.2 Classification

3.5.3.2.1 SVM

SVM is one of the existing popular classifiers in the areas of medical image processing and is good for binary classification. A supervised SVM is a machine learning approach to solve classification and regression issues. It has a the ability to handle large number of features spaces, over fitting can be reduced using soft margin approach, possible to select features as well. However, it is sensitive to noise.

The aim of SVM is to find a best plane to separate data. SVM can be classified as

i) Linear → when data are linearly divided.

ii) Non-linear → when data are not linearly divided and therefore; need an extension of feature sets.

iii) Quadratic → use of kernel tricks.

Two sets of data are necessary for SVM classifier which includes:

1) Train set and
2) Test set

Although SVM is good to find out a perfect boundary however sometimes it can case over fitting. A soft margin parameter can reduce this issue while allowing a small number of points on the wrong side of the boundary, diminishing training accuracy. For a given date set, a kernel function is required which maps the data into a liner distinguishable set.

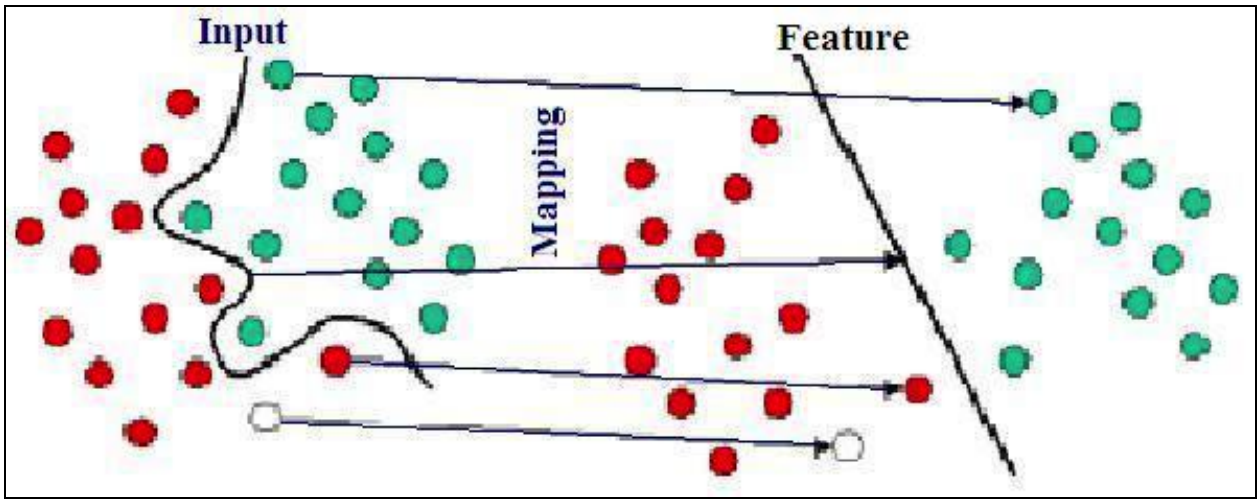

Figure 3-4: Kernel function and mapping

Choice of kernel:

a) Typically default one is Gaussian kernel.
b) If the default is not suitable then it is required to use decorative kernel.
c) Domain experts can assist to formulate the similarity measures (for this research study domain expert is available).

Choice of kernel parameters (σ for Gaussian kernel):

In machine learning classifying data is a common task. Support vector machines or simply SVM is a supervised learning algorithm generally where data analysis is carried out for classification. For a given set of training examples, an SVM training algorithm builds a model that assigns new examples to one category or the other as a fact that SVM is a non-probabilistic binary linear classifier. An SVM model is an illustration of the examples so that the examples of the separate categories are divided by a clear gap that is as wide as possible. New examples are then mapped into that same space and predicted to belong to a category based on the trained set data information.

Using a kernel trick SVM can efficiently perform a non-linear classification in compare to linear classification while completely mapping their inputs into high-dimensional feature spaces.

For a set of unlabeled data supervised learning is practically not possible. In this situation an unsupervised learning approach is essential as a fact that this unsupervised learning approach will attempt to perform a natural clustering of the data to groups and then mapping will takes place to form groups.

There are many hyperplanes can be used to classify the data. The most viable hyperplane is the one which can represent the largest separation or margin between the two classes.

A support vector machine builds a hyperplane or a set of hyperplanes in a high or infinite-dimensional space which can be used for classification. A good separation can be achieved by using the hyperplane which has the largest distance to the nearest training-data point of any class as in general the larger the margin the lower the generalization error of the classifier.

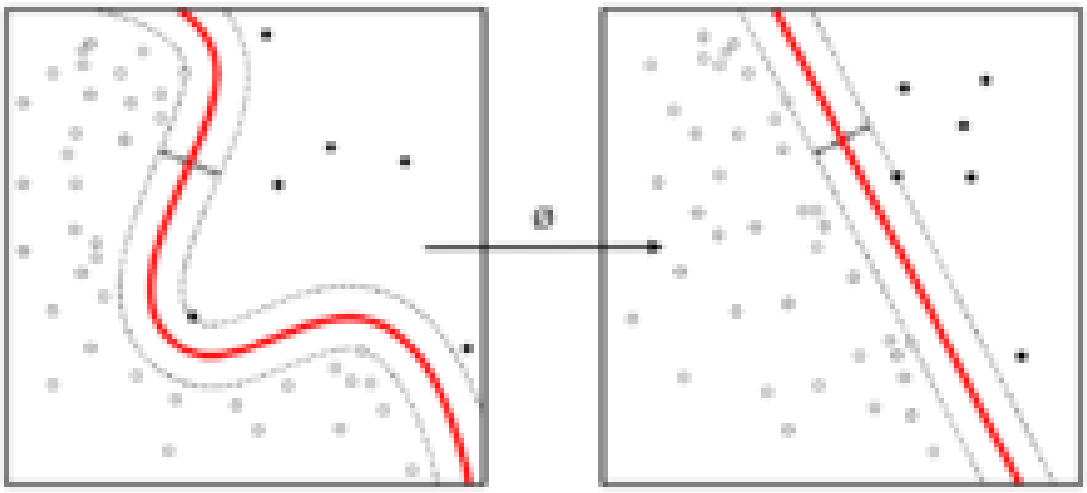

Figure 3-5: Kernel machine

3.5.3.2.2 Naïve Bayes (NB)

Naive Bayes is a supervised as well as statistical machine learning algorithm for classification. It is based on Bayes' probability theorem to predict the class of unknown data set. It predicts membership probabilities for each class such as the probability that given record or data point belongs to a particular class. The class with the highest probability is considered as the most likely class. It actually assumes the presence of a specific feature of a class unrelated to any other feature. For solving multi-class prediction problems, Naïve Bayes is much suitable and it requires much less training data. This method requires only a small amount of training data to guess the parameters which are required for classification. The time taken for training and classification is less and gives real- time prediction.

The main reason for using this algorithm is it assumes that the features incidences are not dependent of each other. As in most fields that deal with events under randomness, probability considerations become significantly effective due toindependence on the occurrence of the extracted features. The extracted features matrix is subjected to be trained in the Naïve Bayes classifier so that it could predict the test image whether it is normal or tumor. Falser tumor objects are trained than tumor objects for better performance since the false tumors are detected in different locations.

3.5.3.2.3 Convolutional Neural Network (CNN)

Convolutional Neural Network is a category of Neural Network which is proved to be very effective in case of image recognition and classification. CNN dominates computer vision techniques because of the accurateness for image classification. CNN is a class of deep, feed-forward artificial neural networks (where connections between nodes do not form a cycle) & use a variation of multi-layer perceptron designed to require minimal pre-processing.

Convolutional Neural Networks is different than regular Neural Networks. In regular Neural Networks input is transformed by putting through a series of hidden layers. Every layer is made up of a set of neurons, where each layer is fully connected to all neurons in the layer before. Neurons in a single layer function completely individually and do not take part in any connections between themselves. Finally, there is a last fully-connected output layes which predicts the result. Regular Neural Networks do not scale well to full images. In case of CNN, the layers are organized in three extents: width, height and depth. It will take 3D input volume to 3D output volume. Further, the neurons in one layer do not connect to all the neurons in the next layer. They are connected to a small region. Lastly, the final output will be reduced to a single vector of probability scores, organized along the depth dimension. Moreover, CNNs perform convolution operation in case of matrix multiplication.

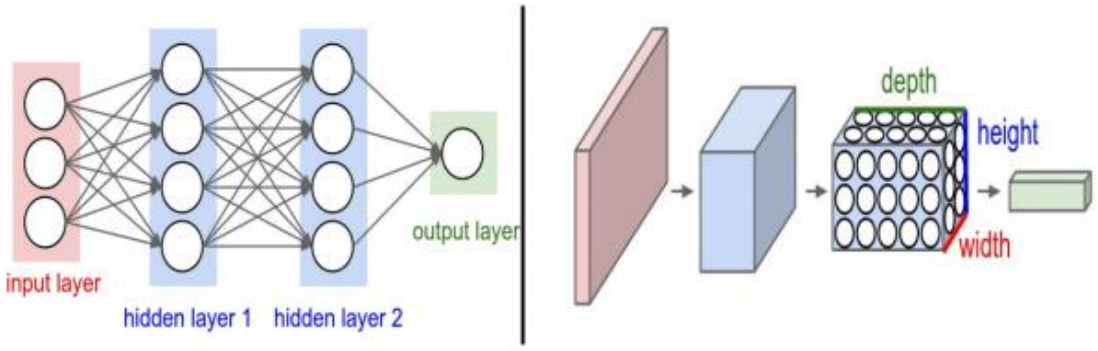

Figure 3-6: A simple Neural Network and Convolutional Neural Network

The CNN based brain tumor classification can be divided into two stages, for example: training and testing stages. In the training phase, preprocessing, feature exaction and classification with Loss function is performed to make a prediction model. Finally, the convolution neural network is used for automatic brain tumor classification.

3.5.3.2.4 Decision Tree

Decision tree is one of the simplest and most fruitful forms of machine learning.A decision tree represents a function that takes a vector of attribute values as input and returns a "decision"—a single output value. The input and output values can be discrete or continuous. After performing a sequence of tests, a decision tree reaches to its decision. Each internal node in tree represents a test of the value on an attribute, each branch represents the outcome of the test and each leaf node represents a class label which is the taken decision after computing all attributes. For decision analysis, a decision tree is used as analytical and visual tool that how the expected values or alternatives are considered. Decision tree can be considered as either classification decision tree or regression decision tree. If the output is one of the finite set of values, the tree is modeled as classification decision tree. If there are only two values then it is called binary of Boolean classification. Regression trees are represented in the same manner; just they predict continuous values like price of a house.

To model a tree it is required to know which features and conditions to choose for splitting and when to stop. If dataset is available, then it is really important to learn about it to classify it in an optimal way. Decision tree always takes decision at each point and splits the data set depending on that decision. It is a top down traversal and each split should provide the maximum information. If the dataset is huge and also there are many features then it is important to find out the best features to split the data set for efficient and optimal classification.

3.6 Data Analysis Techniques

This study incorporated MRI brain tumour grayscale images. Data analysis techniques for this study images are based on

(1) Selection criteria of analysis and

(2) Evaluation of results

3.6.1 Selection Criteria of Analysis

There are three types of analysis were considered in this study. The selections of the methods included were based on three types of criteria which are as follows.

(1) The first criteria used basic image processing techniques using conventional ML.

(2) The second criteria used existing research works mentioned in literature review.

(3) Third criteria is to add/modify the where necessary to get the most accurate results to identify the brain tumor cells.

The primary goal of this research study is to apply computerized algorithms to analyze and identify the brain tumor tissues acquired from MRI scanners.

3.6.2 Evaluation of Results

Finally the results were evaluated with experts marked results. Validations of results are discussed in chapter 4.

3.7 Summary

In this chapter this study research dataset and methodology for MRI brain tumor cell analysis has been explained. The computerized image processing approach was divided into two phases and each phase consist a number of steps. In the literature there are a number of techniques that can be incorporated as a technique for each step which were explained in this chapter. In total there were 2 different approaches were incorporated using various techniques and modifications if available techniques where necessary for this research study from where proposed approach was selected based on the results accuracy rate in compare to experts' manual test results. Results were validated through comparison with pathology experts' manual test results.

CHAPTER 4

EXPERIMENTAL RESULTS

This chapter describes Research Activity 1 that has been employed to conduct research using Conventional ML. In total two different approaches employed in this Research Activity 1. To perform these 2 different approaches 4 test images were used. Then onwards, this chapter includes Research Activity 2 which conducted research using Deep ML. Finally the chapter concludes with details of the chapter summary.

4.1 Research Activity 1 (Conventional ML)

This activity explored the existing available approaches for this research study test images to identify brain tumour tissues acquired from MRI images. To assess the images processing approaches and to propose a suitable image processing approach for this research study test images 2 different approaches were incorporated which are described below.

4.1.1 Research Approach One

This is the basic and most widely used image analysis approach for medical tissue image processing. The diagram of research approach one is shown in Figure 4-1. Research approach one has two phases where phase one include

i) Filter operation and

ii) Grayscale segmentation

and phase two include

i) Identification of tumour region

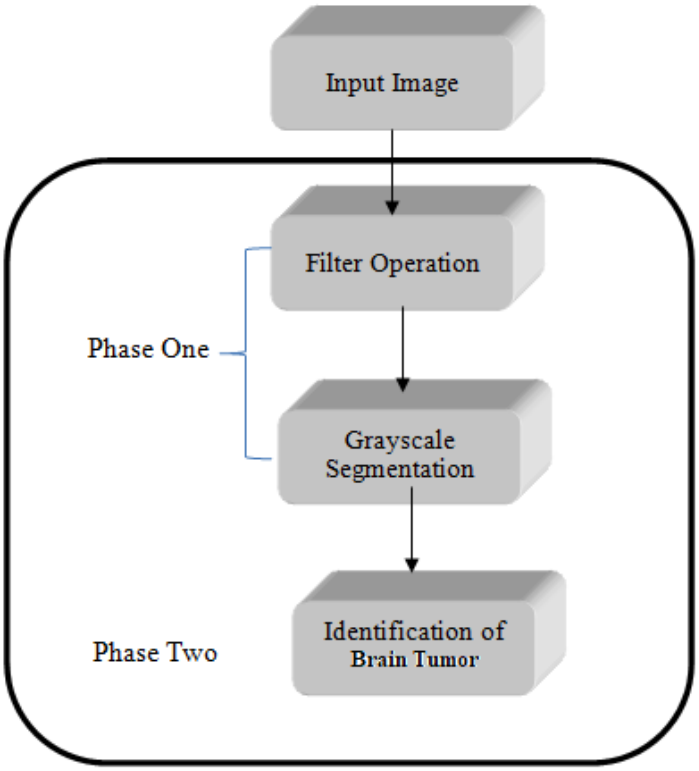

Figure 4-1: Detailed flow-chart for research approach one

There are a number of filter operations available mentioned in the literature. Different types of filter operations used in this research approach one which include

(a) Gaussian filter,

(b) Median filter, and

(c) Morphological filter.

For basic image processing approach gray-scale segmentation is the most popular one and threshold based segmentation technique is mostly used. During gray-scale segmentation color image converts to gray-scale image. For gray-scale images color feature does not work. Shape and size features would be applicable.

4.1.2 Research Approach Two

This is the basic and most widely used image analysis approach for medical tissue image processing. The diagram of research approach one is shown in Figure 4-2. Research approach one has two phases where phase one include

i) Filter operation with enhancement and

ii) Grayscale segmentation

and phase two include

i) Identification of tumour region

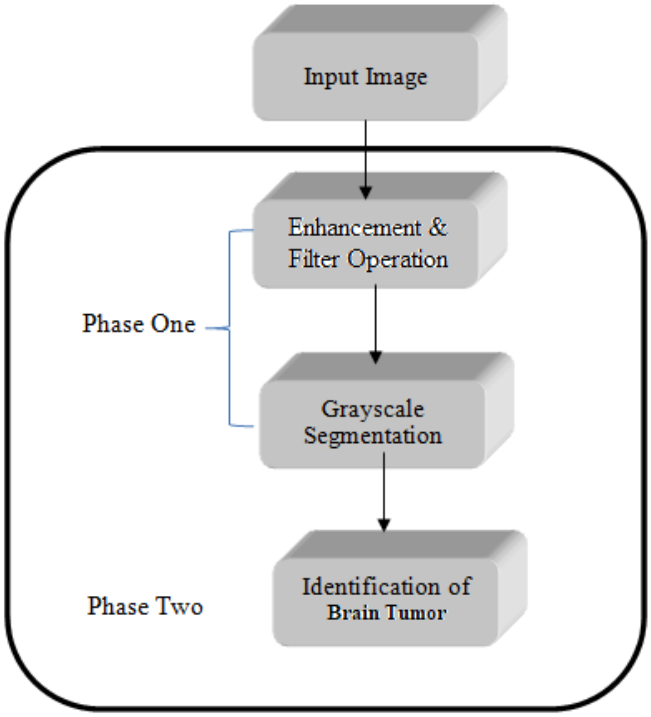

Figure 4-2: Detailed flow-chart for research approach two

There are a number of filter operations available mentioned in the literature. Different types of filter operations used in this research approach one which include

(a) Gaussian filter,

(b) Median filter, and

(c) Morphological filter.

For basic image processing approach gray-scale segmentation is the most popular one and threshold based segmentation technique is mostly used. During gray-scale segmentation color image converts to gray-scale image. For gray-scale images color feature does not work. Shape and size features would be applicable.

Figure 4-3 to 4-6 indicates the results of filter operation where Gaussian filer, Median filter and morphological filter were used. In addition to that Figure 4-3 to 4-6 indicates a comparative results between research approach one and research approach where for research approach one incorporated filter, segmentation and identification and research approach to incorporated filter with enhancement, segmentation and identification. Figure 4-7 to 4-10 indicates the results of segmentation using OTSU threshold segmentation approach applied for both research approach one (without enhancement) and research approach two (with enhancement). Finally Figure 4-11 to 4-14 are the results of identified regions of brain tumour for both research approach one and research approach two where from research approach one enhancement was not included but for research approach two enhancement was incorporated.

4.1.3 Experiment Results

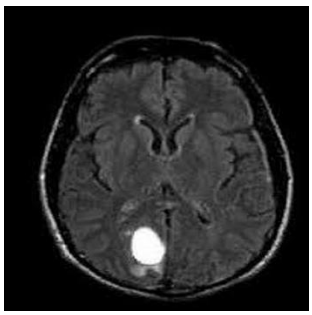

(a) MRI Brain tumour test image [1]

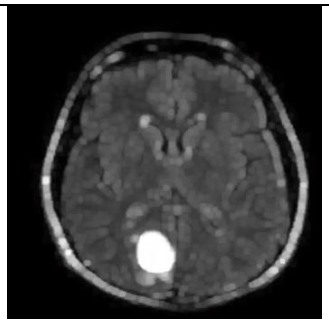

(b) Test image (a) was filtered using Gaussian filter (without enhancement)

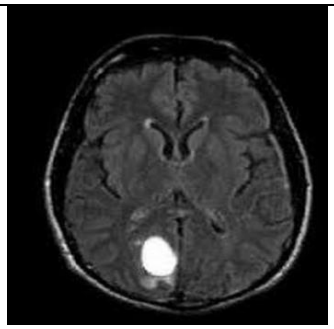

(c) Test image (a) was filtered using Gaussian filter (with enhancement)

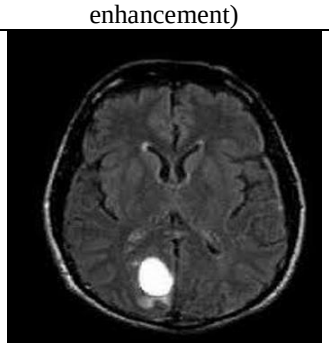

(d) Test image (a) was filtered using Median filter (without enhancement)

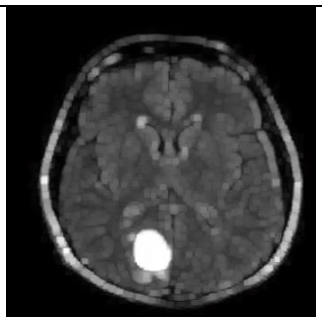

(e) Test image (a) was filtered using Median filter (with enhancement)

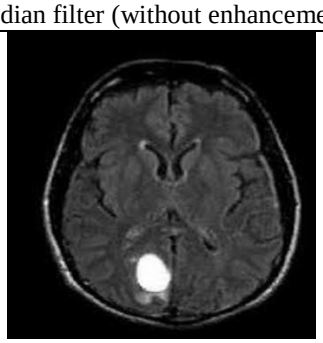

(f) Test image (a) was filtered using Morphological Operation (without enhancement)

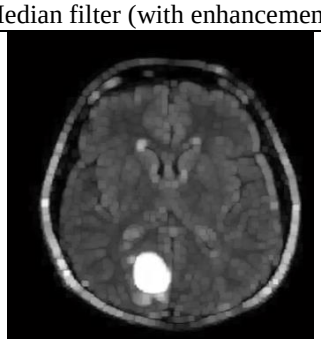

(g) Test image (a) was filtered using Morphological Operation (with enhancement)

Figure 4-3: Filter operation using Gaussian filter, Median filter and Morphological Operation (image (a) test MRI brain tumor image, image (b) filtered image using Gaussian filter (without enhancement), image (d) filtered image using Median filter (without enhancement), image (f) filtered image using Morphological Operation (without enhancement), image (c) filtered image using Gaussian filter (with enhancement), image (e) filtered image using Median filter (with enhancement), image (g) filtered image using Morphological Operation (with enhancement).

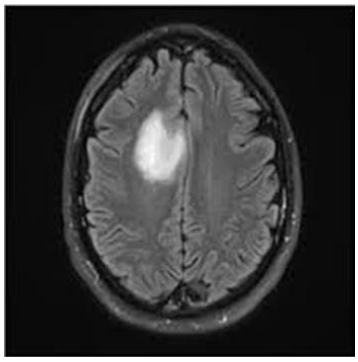

(a) MRI Brain tumour test image [2]

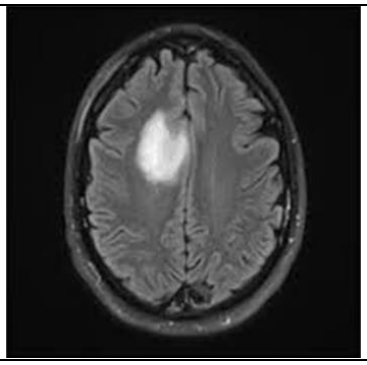

(b) Test image (a) was filtered using Gaussian filter (without enhancement)

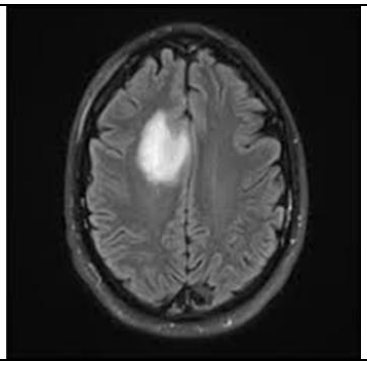

(c) Test image (a) was filtered using Gaussian filter (with enhancement)

(d) Test image (a) was filtered using Median filter (without enhancement)

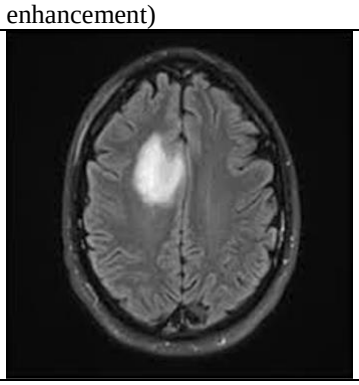

(e) Test image (a) was filtered using Median filter (with enhancement)

(f) Test image (a) was filtered using Morphological Operation (without enhancement)

(g) Test image (a) was filtered using Morphological Operation (with enhancement)

Figure 4-4: Filter operation using Gaussian filter, Median filter and Morphological Operation (image (a) test MRI brain tumor image, image (b) filtered image using Gaussian filter (without enhancement), image (d) filtered image using Median filter (without enhancement), image (f) filtered image using Morphological Operation (without enhancement), image (c) filtered image using Gaussian filter (with enhancement), image (e) filtered image using Median filter (with enhancement), image (g) filtered image using Morphological Operation (with enhancement).

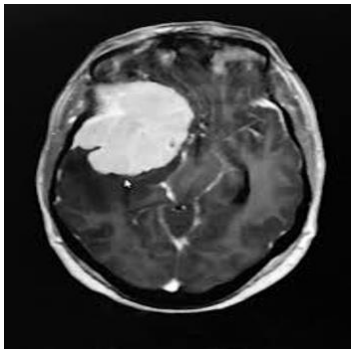

(a) MRI Brain tumour test image [3]

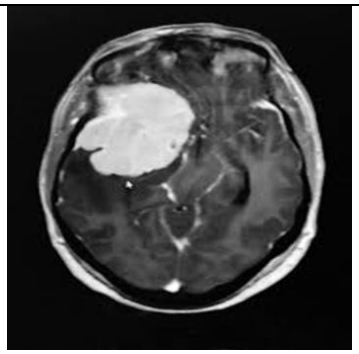

(b) Test image (a) was filtered using Gaussian filter (without enhancement)

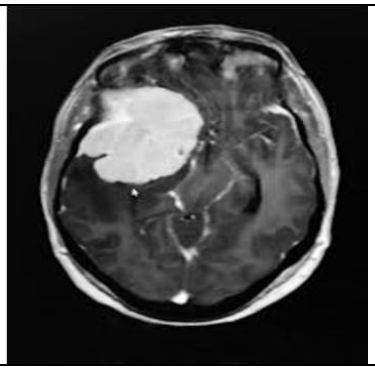

(b) Test image (a) was filtered using Gaussian filter (with enhancement)

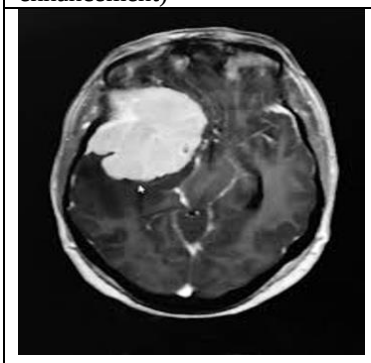

(c) Test image (a) was filtered using Median filter (without enhancement)

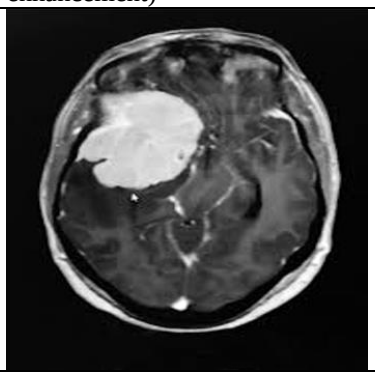

(c) Test image (a) was filtered using Median filter (with enhancement)

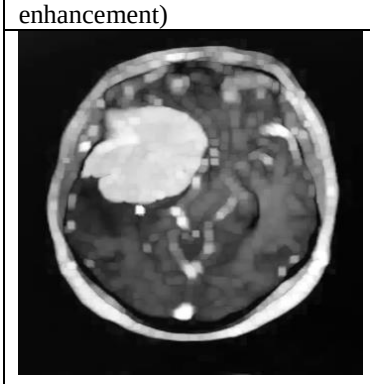

(d) Test image (a) was filtered using Morphological Operation (without enhancement)

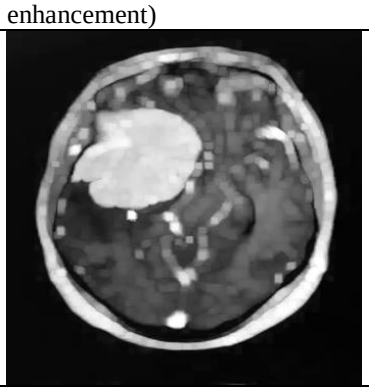

(d) Test image (a) was filtered using Morphological Operation (with enhancement)

Figure 4-5: Filter operation using Gaussian filter, Median filter and Morphological Operation (image (a) test MRI brain tumor image, image (b) filtered image using Gaussian filter (without enhancement), image (d) filtered image using Median filter (without enhancement), image (f) filtered image using Morphological Operation (without enhancement), image (c) filtered image using Gaussian filter (with enhancement), image (e) filtered image using Median filter (with enhancement), image (g) filtered image using Morphological Operation (with enhancement).

(a) MRI Brain tumour test image [4]

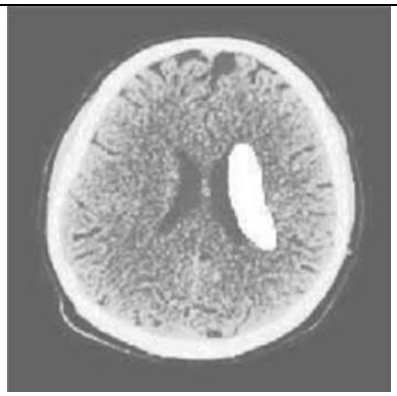

(b) Test image (a) was filtered using Gaussian filter (without enhancement)

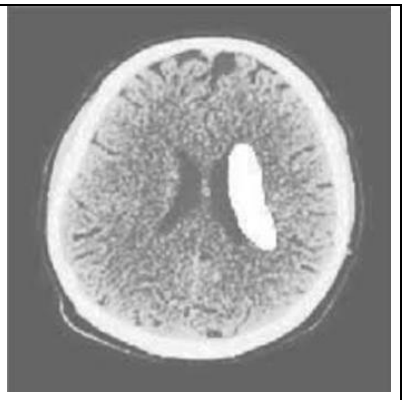

(b) Test image (a) was filtered using Gaussian filter (with enhancement)

(c) Test image (a) was filtered using Median filter (without enhancement)

(c) Test image (a) was filtered using Median filter (with enhancement)

(d) Test image (a) was filtered using Morphological Operation (without enhancement)

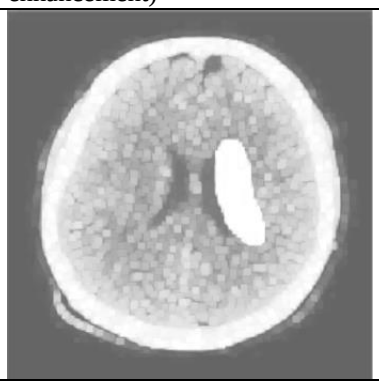

(d) Test image (a) was filtered using Morphological Operation (with enhancement)

Figure 4-6: Filter operation using Gaussian filter, Median filter and Morphological Operation (image (a) test MRI brain tumor image, image (b) filtered image using Gaussian filter (without enhancement), image (d) filtered image using Median filter (without enhancement), image (f) filtered image using Morphological Operation (without enhancement), image (c) filtered image using Gaussian filter (with enhancement), image (e) filtered image using Median filter (with enhancement), image (g) filtered image using Morphological Operation (with enhancement).

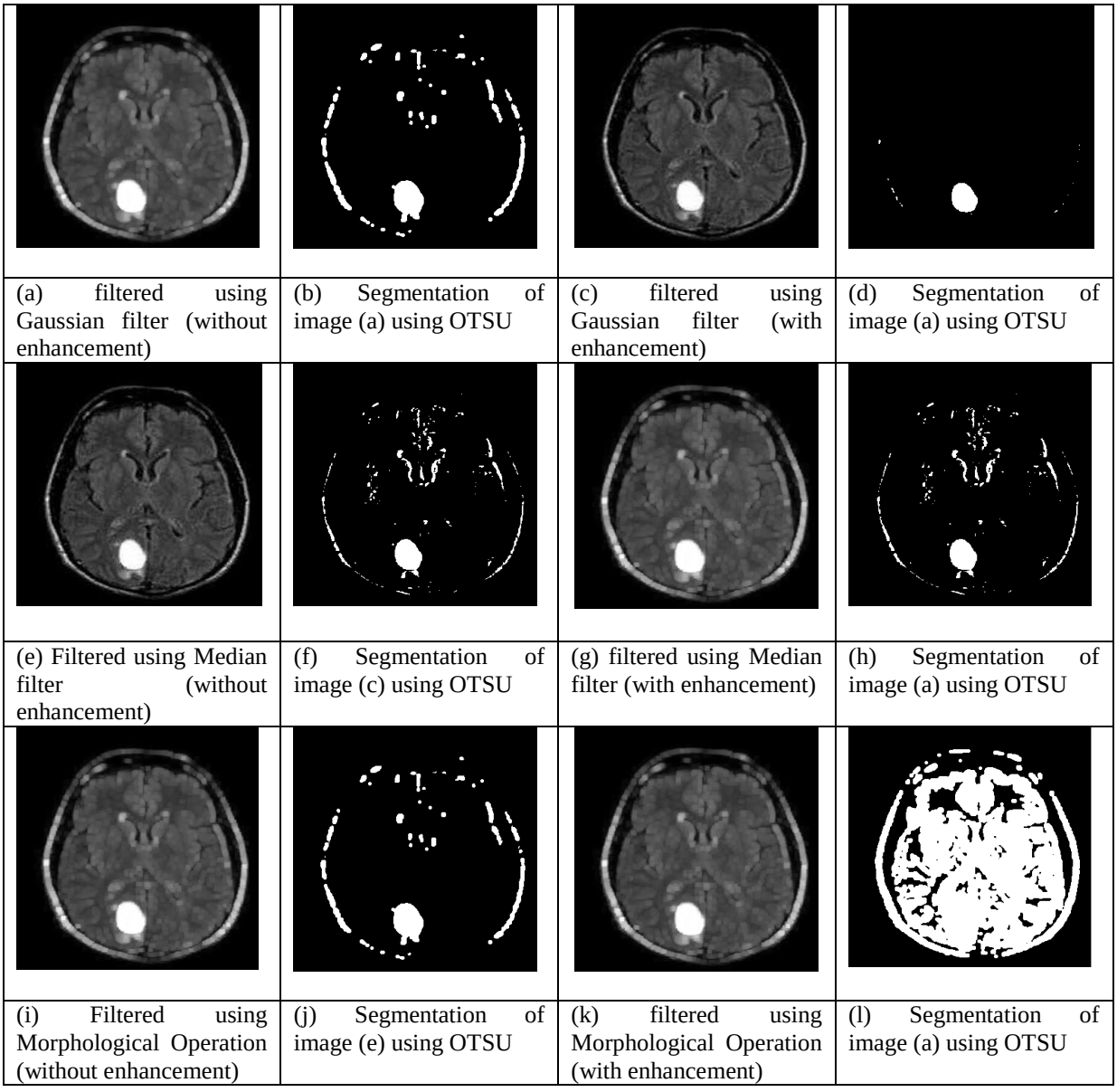

(a) filtered using Gaussian filter (without enhancement)	(b) Segmentation of image (a) using OTSU	(c) filtered using Gaussian filter (with enhancement)	(d) Segmentation of image (a) using OTSU
(e) Filtered using Median filter (without enhancement)	(f) Segmentation of image (c) using OTSU	(g) filtered using Median filter (with enhancement)	(h) Segmentation of image (a) using OTSU
(i) Filtered using Morphological Operation (without enhancement)	(j) Segmentation of image (e) using OTSU	(k) filtered using Morphological Operation (with enhancement)	(l) Segmentation of image (a) using OTSU

Figure 4-7: (a) Filtered image using Gaussian filter (without enhancement), (e) using Median filter (without enhancement) and (i) Morphological Operation (without enhancement). (b), (f) and (j) are segmented images for image (a), (e) and (i). (c) Filtered image using Gaussian filter (with enhancement), (g) using Median filter (with enhancement) and (k) Morphological Operation (with enhancement). (d), (h) and (l) are segmented images for image (c), (g) and (k). [test image 1]

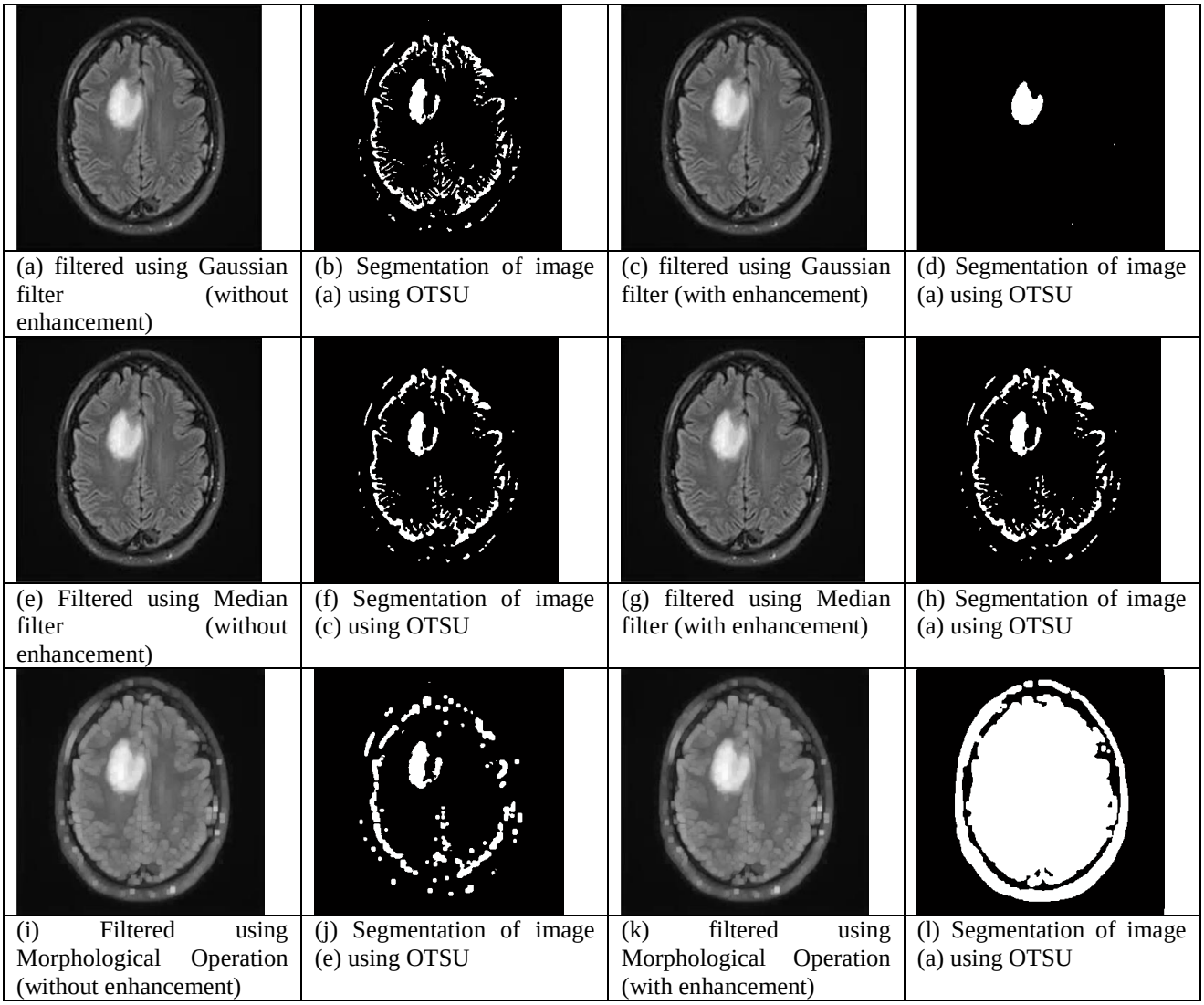

(a) filtered using Gaussian filter (without enhancement)	(b) Segmentation of image (a) using OTSU	(c) filtered using Gaussian filter (with enhancement)	(d) Segmentation of image (a) using OTSU
(e) Filtered using Median filter (without enhancement)	(f) Segmentation of image (c) using OTSU	(g) filtered using Median filter (with enhancement)	(h) Segmentation of image (a) using OTSU
(i) Filtered using Morphological Operation (without enhancement)	(j) Segmentation of image (e) using OTSU	(k) filtered using Morphological Operation (with enhancement)	(l) Segmentation of image (a) using OTSU

Figure 4-8: (a) Filtered image using Gaussian filter (without enhancement), (e) using Median filter (without enhancement) and (i) Morphological Operation (without enhancement). (b), (f) and (j) are segmented images for image (a), (e) and (i). (c) Filtered image using Gaussian filter (with enhancement), (g) using Median filter (with enhancement) and (k) Morphological Operation (with enhancement). (d), (h) and (l) are segmented images for image (c), (g) and (k). [test image 2]

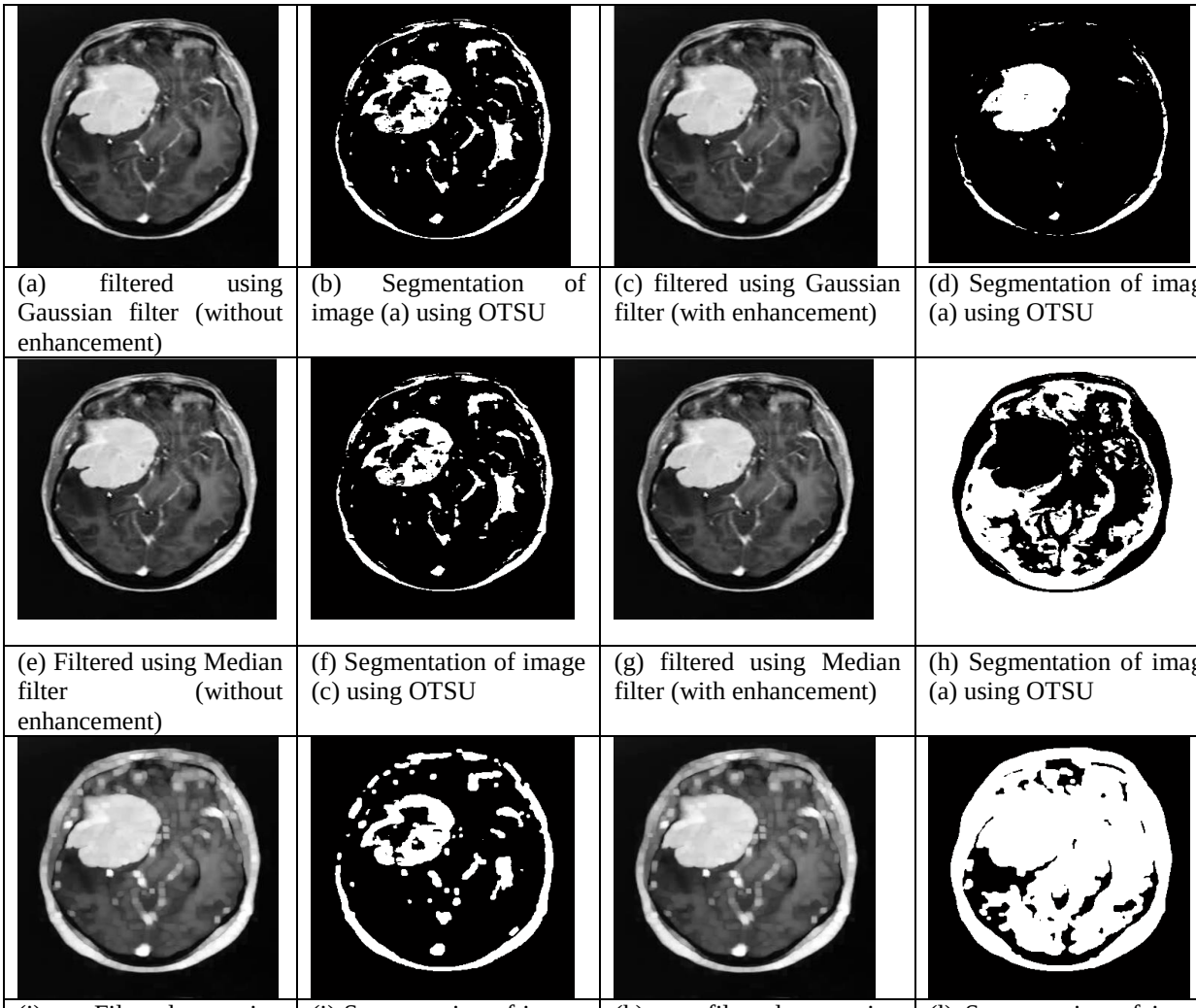

(a) filtered using Gaussian filter (without enhancement)	(b) Segmentation of image (a) using OTSU	(c) filtered using Gaussian filter (with enhancement)	(d) Segmentation of image (a) using OTSU
(e) Filtered using Median filter (without enhancement)	(f) Segmentation of image (c) using OTSU	(g) filtered using Median filter (with enhancement)	(h) Segmentation of image (a) using OTSU
(i) Filtered using Morphological Operation (without enhancement)	(j) Segmentation of image (e) using OTSU	(k) filtered using Morphological Operation (with enhancement)	(l) Segmentation of image (a) using OTSU

Figure 4-9: (a) Filtered image using Gaussian filter (without enhancement), (e) using Median filter (without enhancement) and (i) Morphological Operation (without enhancement). (b), (f) and (j) are segmented images for image (a), (e) and (i). (c) Filtered image using Gaussian filter (with enhancement), (g) using Median filter (with enhancement) and (k) Morphological Operation (with enhancement). (d), (h) and (l) are segmented images for image (c), (g) and (k). [test image 3]

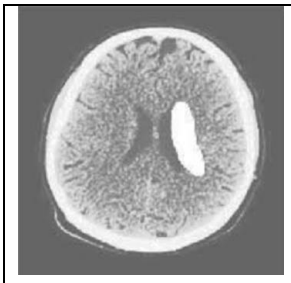		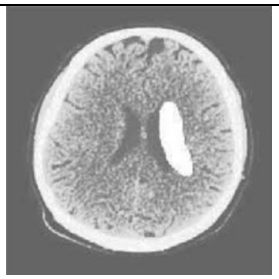	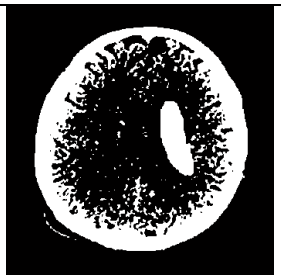
(a) filtered using Gaussian filter (without enhancement)	(b) Segmentation of image (a) using OTSU	(c) filtered using Gaussian filter (with enhancement)	(d) Segmentation of image (a) using OTSU
	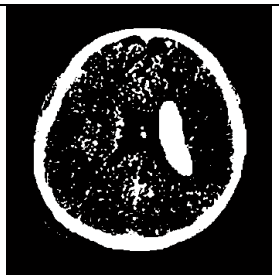	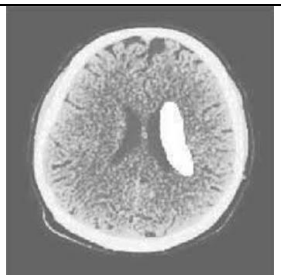	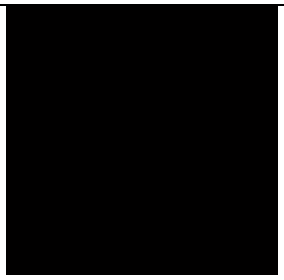
(e) Filtered using Median filter (without enhancement)	(f) Segmentation of image (c) using OTSU	(g) filtered using Median filter (with enhancement)	(h) Segmentation of image (a) using OTSU
	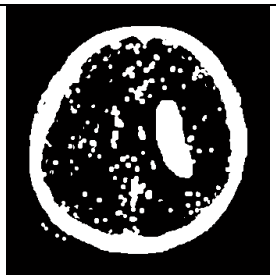	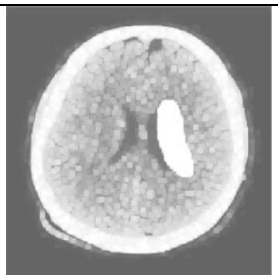	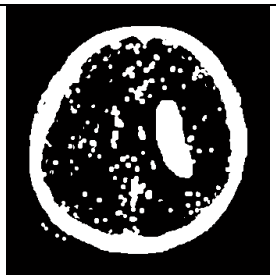
(i) Filtered using Morphological Operation (without enhancement)	(j) Segmentation of image (e) using OTSU	(k) filtered using Morphological Operation (with enhancement)	(l) Segmentation of image (a) using OTSU

Figure 4-10: (a) Filtered image using Gaussian filter (without enhancement), (e) using Median filter (without enhancement) and (i) Morphological Operation (without enhancement). (b), (f) and (j) are segmented images for image (a), (e) and (i). (c) Filtered image using Gaussian filter (with enhancement), (g) using Median filter (with enhancement) and (k) Morphological Operation (with enhancement). (d), (h) and (l) are segmented images for image (c), (g) and (k). [test image 4]

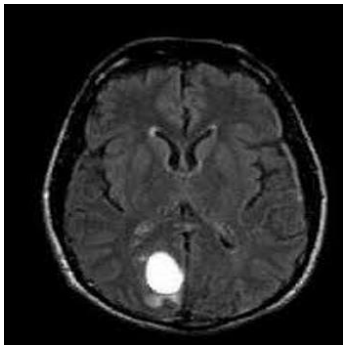

(a) Expert manual analysis result **[test image 1]**

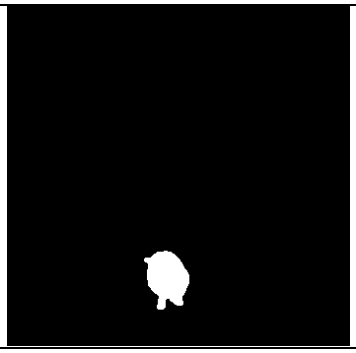

(b) Identified results using Gaussian filter (with enhancement)

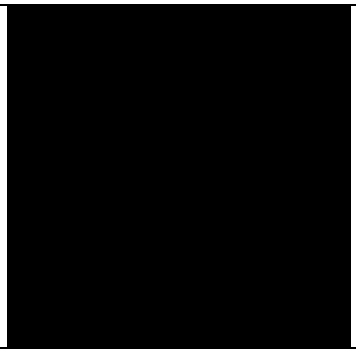

(c) Identified results using Gaussian filter (without enhancement)

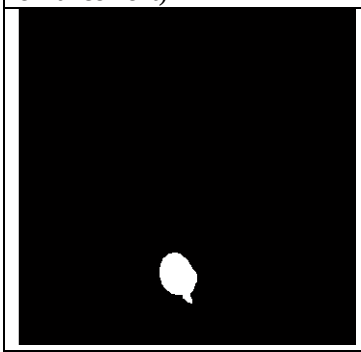

(d) Identified results using Median filter (with enhancement)

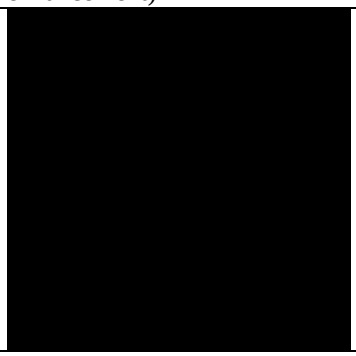

(e) Identified results using Median filter (without enhancement)

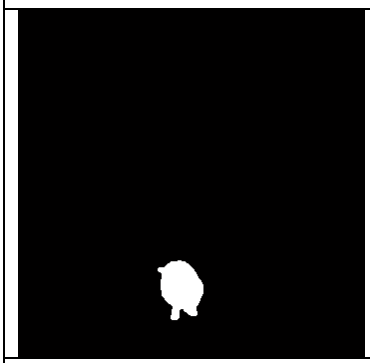

(f) Identified results using Morphological Operation (with enhancement)

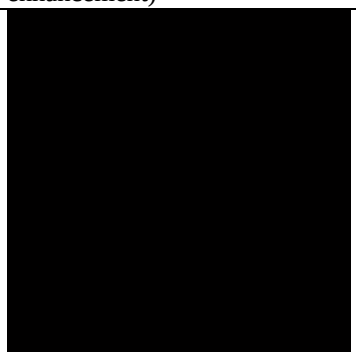

(g) Identified results using Morphological Operation (without enhancement)

Figure 4-11: Identification of results for research approach one and research approach two

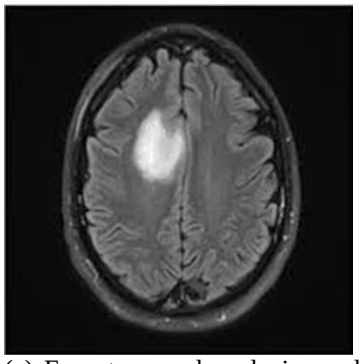

(a) Expert manual analysis result **[test image 2]**

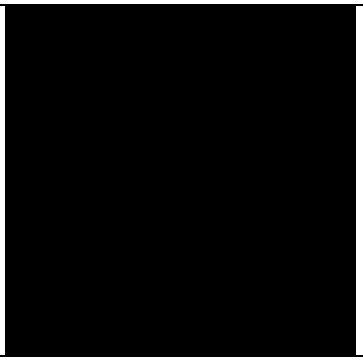

(b) Identified results using Gaussian filter (with enhancement)

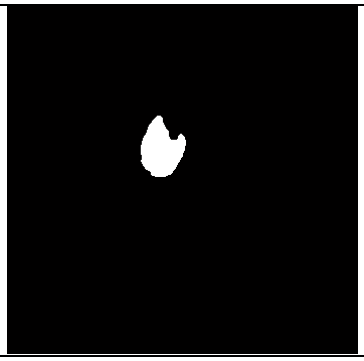

(c) Identified results using Gaussian filter (without enhancement)

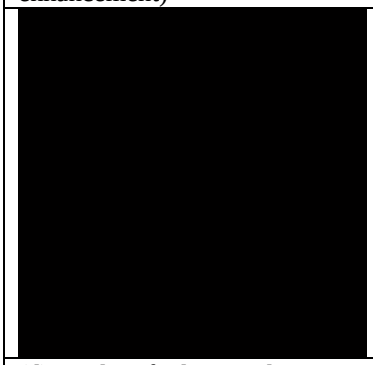

(d) Identified results using Median filter (with enhancement)

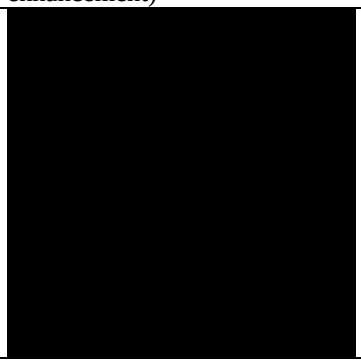

(e) Identified results using Median filter (without enhancement)

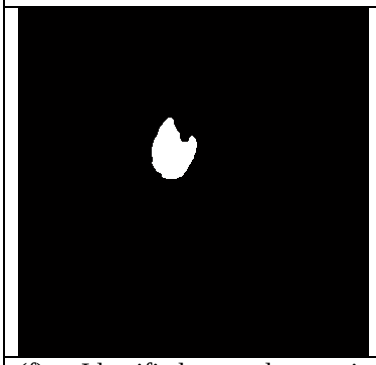

(f) Identified results using Morphological Operation (with enhancement)

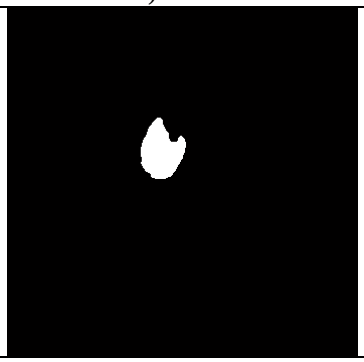

(g) Identified results using Morphological Operation (without enhancement)

Figure 4-12: Identification of results for research approach one and research approach two

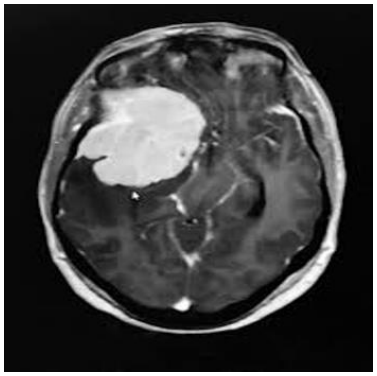

(a) Expert manual analysis result **[test image 3]**

(b) Identified results using Gaussian filter (with enhancement)

(c) Identified results using Gaussian filter (without enhancement)

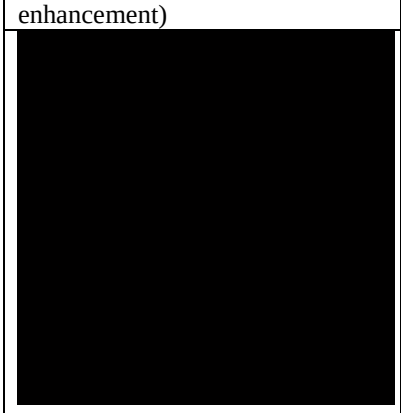

(d) Identified results using Median filter (with enhancement)

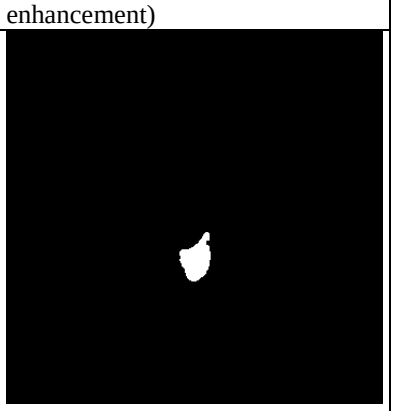

(e) Identified results using Median filter (without enhancement)

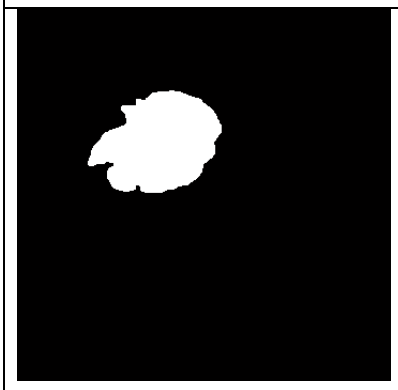

(f) Identified results using Morphological Operation (with enhancement)

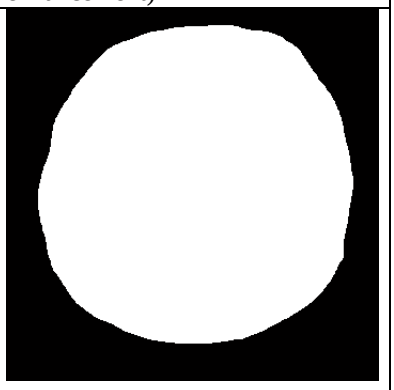

(g) Identified results using Morphological Operation (without enhancement)

Figure 4-13: Identification results for research approach one and research approach two

(a) Expert manual analysis result **[test image 4]**

(b) Identified results using Gaussian filter (with enhancement)

(c) Identified results using Gaussian filter (without enhancement)

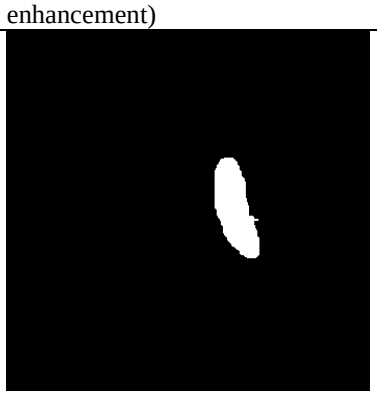

(d) Identified results using Median filter (with enhancement)

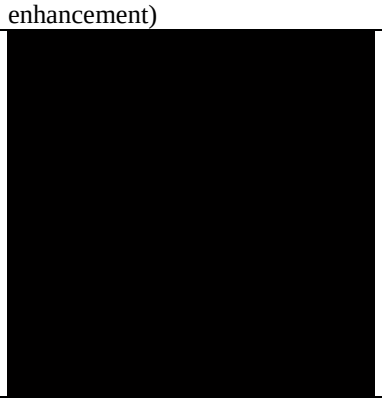

(e) Identified results using Median filter (without enhancement)

(f) Identified results using Morphological Operation (with enhancement)

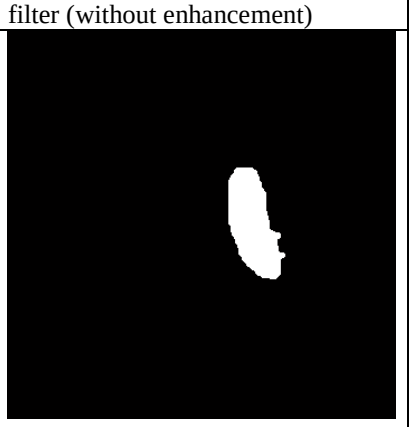

(g) Identified results using Morphological Operation (without enhancement)

Figure 4-14: Identification of results for research approach one and research approach two

4.1.4 Summary

The results indicate that identification result accuracy for research approach two (with enhancement) performs better than research approach one (without enhancement). Additionally, filter operation performed using Gaussian filter approach was found lowest accuracy. Identification results using Morphological filter approach was highest in comparison to all three filter approaches used in this research approaches.

All the approaches were tested for MRI brain tumor images. An accuracy rate over 85% which is the “Gold standard” accuracy rate for manual microscopic analysis will be a suitable approach for this research test images. Identified result using Morphological Operation may be a suitable approach for this research study test images as this approach was able to maintain the accuracy rate over 85%.

4.2 Research Activity 2 (Deep ML)

After the successful completion of the above mentioned conventional machine learning approach, deep learning method was implemented to identify the brain tumorous cells from MRI gray scale images. The output of each steps that are followed to achieve the result are given below:

4.2.1 Effects of Filter Size

2D Convolutional layer is applied with 4 different filter sizes-

Filter Size 40

Total 2086 data are used to train the model and then 90 test data are used to test the result.

The result obtained by selecting filter size 40 is shown below:

Model	Accuracy (train)	Precision (train)	Recall (train)	F1_score (train)	Specificity (train)	Accuracy (test)	Precision (test)	Recall (test)	F1_score (test)	Specificity (test)
CNN	1.000	1.000	1.000	1.000	1.000	0.978	0.978	0.978	0.978	0.857

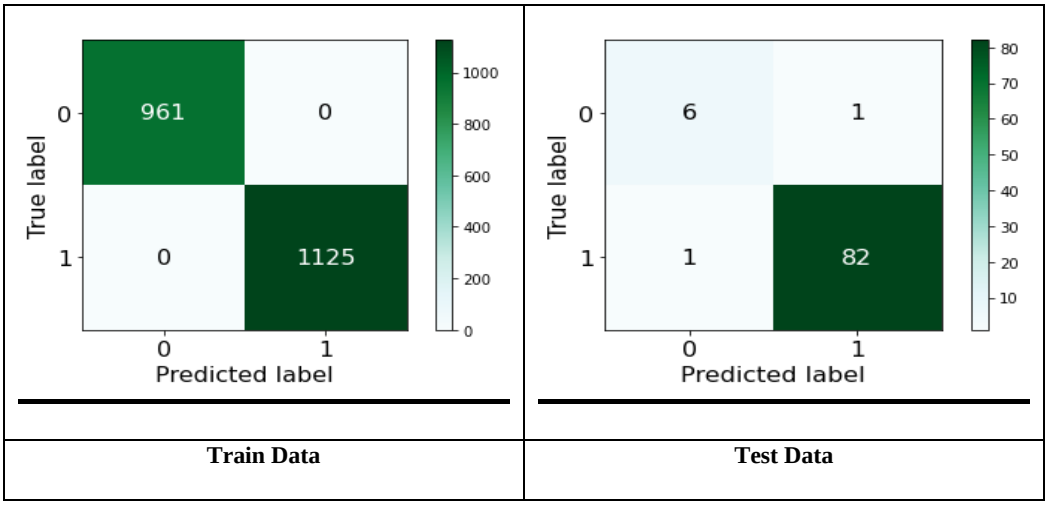

Train Data | **Test Data**

Fig 4-15: Confusion Matrix for selecting filter size 40

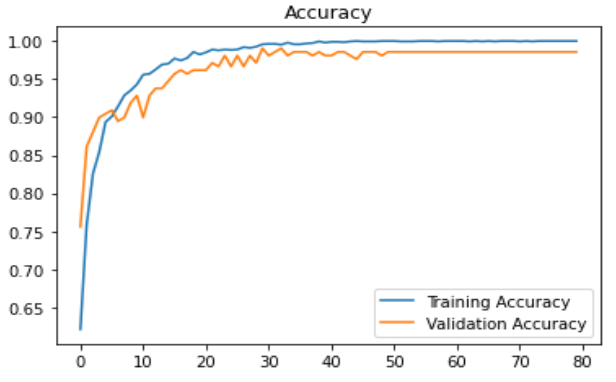

Fig 4-16: Train vs Validation Accuracy for each Epoch for filter size 40

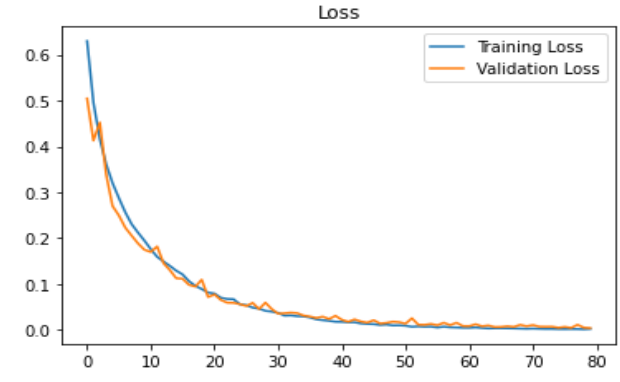

Fig 4-17: Train vs Validation Loss for each Epoch for filter size 40

Filter Size 28

Model	Accuracy (train)	Precision (train)	Recall (train)	F1_score (train)	Specificity (train)	Accuracy (test)	Precision (test)	Recall (test)	F1_score (test)	Specificity (test)
CNN	1.000	1.000	1.000	1.000	1.000	0.944	0.957	0.944	0.949	0.600

The exact same 2086 data are used to train the model and then 90 test data are used to test the result. The result obtained by selecting filter size 28 is shown below:

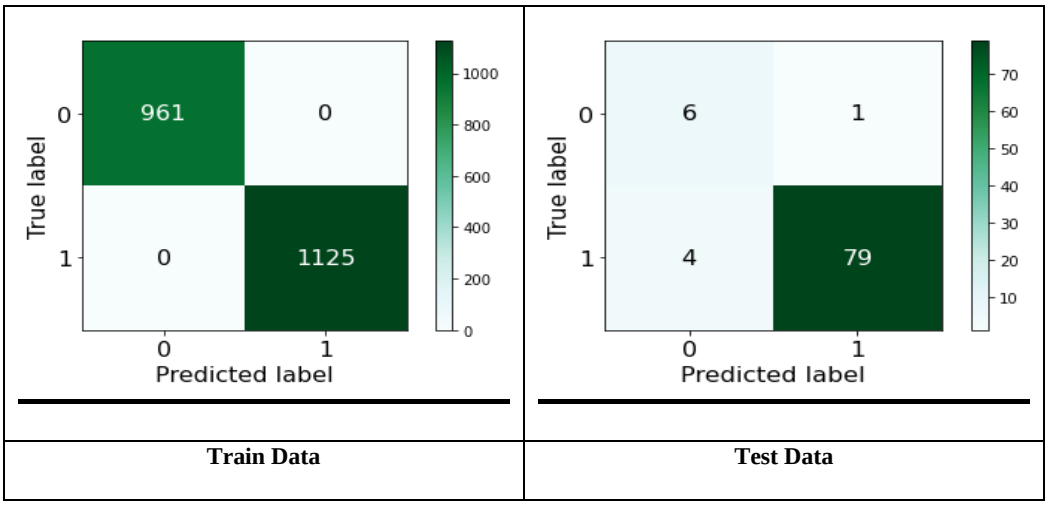

Train Data | **Test Data**

Fig 4-18: Confusion Matrix for selecting filter size 28

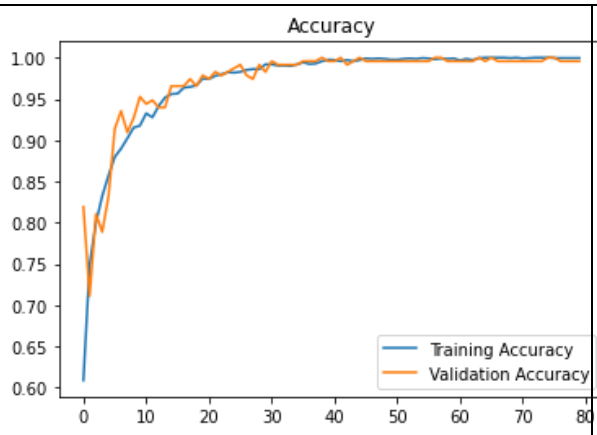

Fig 4-19: Train vs Validation Accuracy for each Epoch for filter size 28

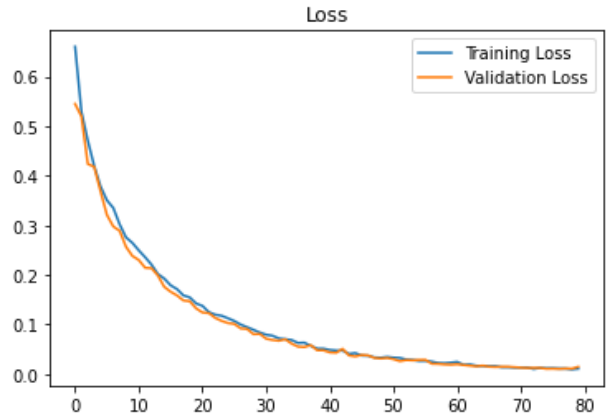

Fig 4-20: Train vs Validation Loss for each Epoch for filter size 28

Filter Size 16

Model	Accuracy (train)	Precision (train)	Recall (train)	F1_score (train)	Specificity (train)	Accuracy (test)	Precision (test)	Recall (test)	F1_score (test)	Specificity (test)
CNN	1.000	1.000	1.000	1.000	1.000	0.978	0.978	0.978	0.978	0.857

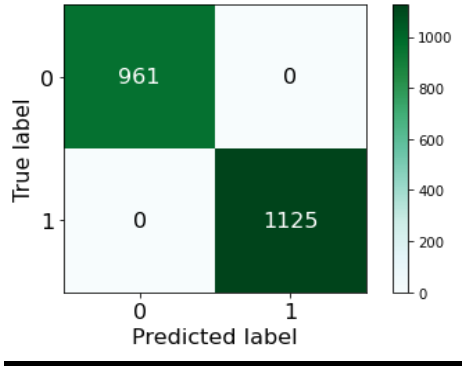

Train Data

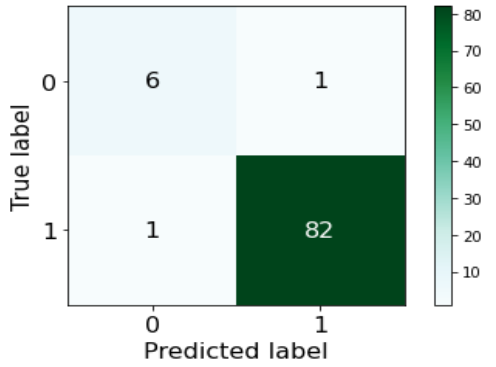

Test Data

Fig 4-21: Confusion Matrix for selecting filter size 16

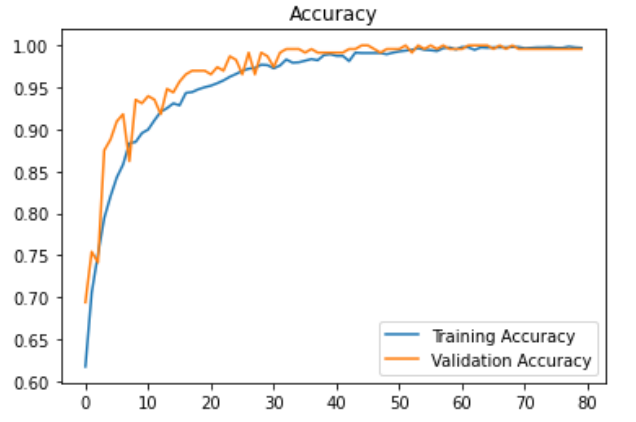

Fig 4-22: Train vs Validation Accuracy for each Epoch for filter size 16

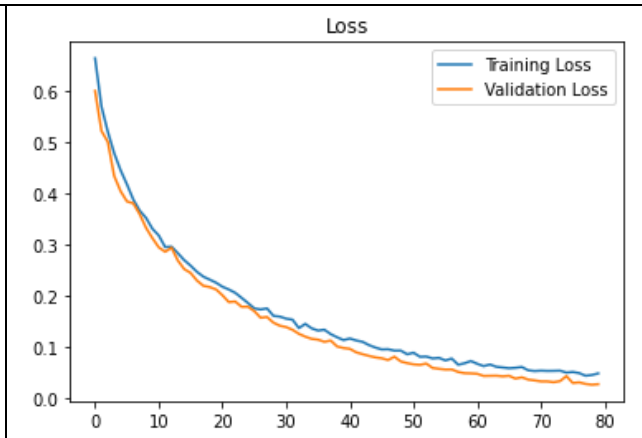

Fig 4-23: Train vs Validation Loss for each Epoch for filter size 16

Filter Size 32 (optimal result)

CNN Model Architecture

Layer (type)	Output Shape	Parameters#
vgg16 (Pre-trained Model)	(None, 7, 7, 512)	14714688
Conv2d (Convolutional layer)	(None, 7, 7, 32)	802848
Max_pooling2d	(None, 1, 1, 32)	0
Dropout (50%)	(None, 1, 1, 32)	0
Flatten layer	(None, 32)	0
Dense layer	(None, 1)	33

Total Parameters: 15,517,569
Trainable Parameters: 802,881
Non-trainable Parameters: 14,714,688

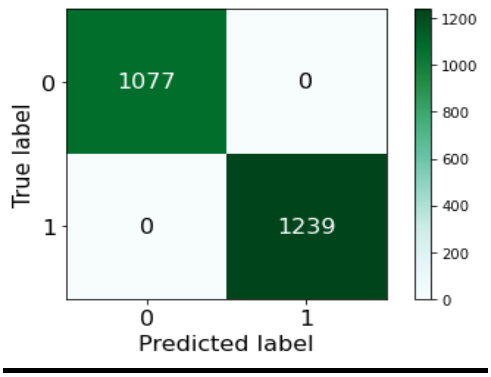

Train Data | **Test Data**

Fig 4-24: Confusion Matrix for selecting filter size 32

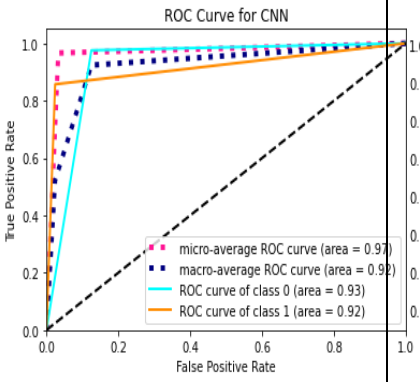

Fig 4-25: Receiver Operating Characteristic (ROC) Curve for CNN

Fig 4-26: Train vs Validation Accuracy for each Epoch for filter size 32

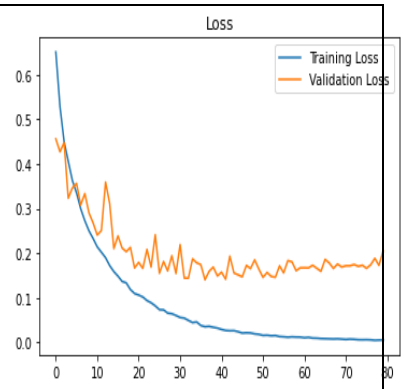

Fig 4-27: Train vs Validation Loss for each Epoch for filter size 32

4.2.2 Effects of Threshold Function

ReLU (Rectified Lineal Unit) as Activation Function in Dense Layer

Model	Accuracy (train)	Precision (train)	Recall (train)	F1_score (train)	Specificity (train)	Accuracy (test)	Precision (test)	Recall (test)	F1_score (test)	Specificity (test)
CNN	1.000	1.000	1.000	1.000	1.000	0.967	0.969	0.967	0.968	0.750

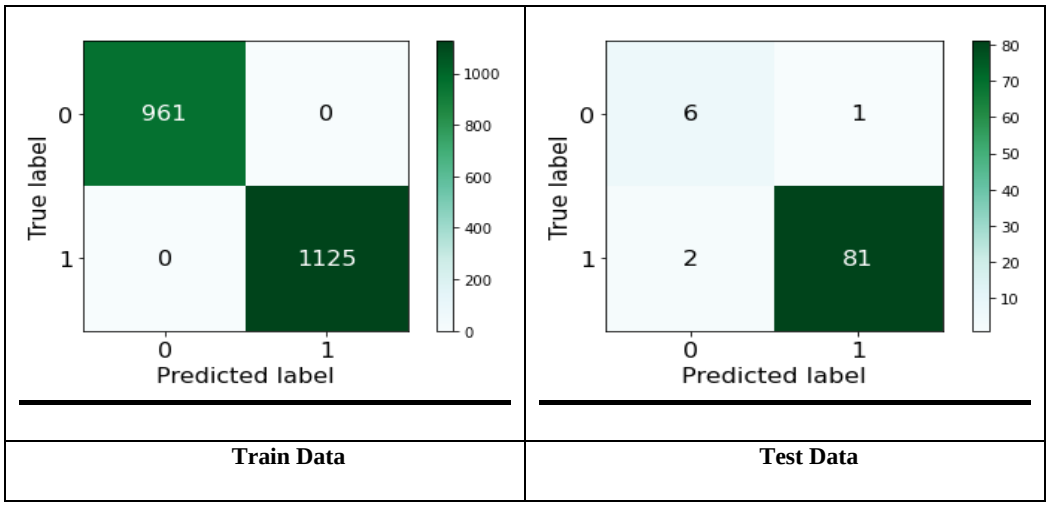

Train Data | **Test Data**

Fig 4-28: Confusion Matrix after selecting ReLU activation function in dense layer

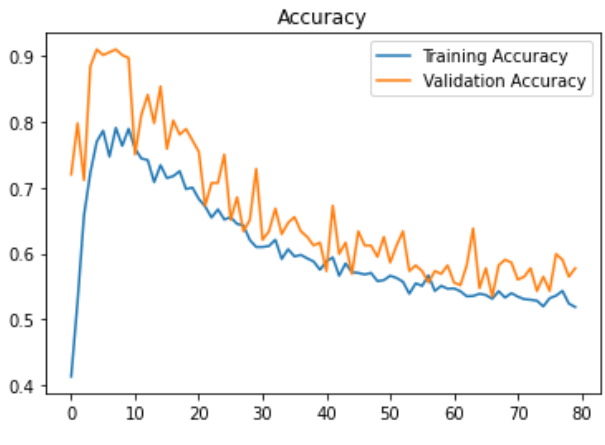

Fig 4-29: Train vs Validation Accuracy for each Epoch after selecting ReLU activation function in dense layer

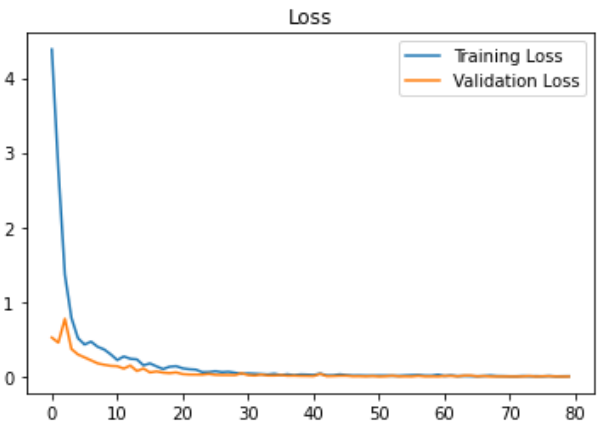

Fig 4-30: Train vs Validation Loss for each Epoch after selecting ReLU activation function in dense layer

Softmax as Aactivation Function in Dense Layer

Model	Accuracy (train)	Precision (train)	Recall (train)	F1_score (train)	Specificity (train)	Accuracy (test)	Precision (test)	Recall (test)	F1_score (test)	Specificity (test)
CNN	0.539	0.291	0.39	0.378	N/A	0.922	0.850	.922	0.855	N/A

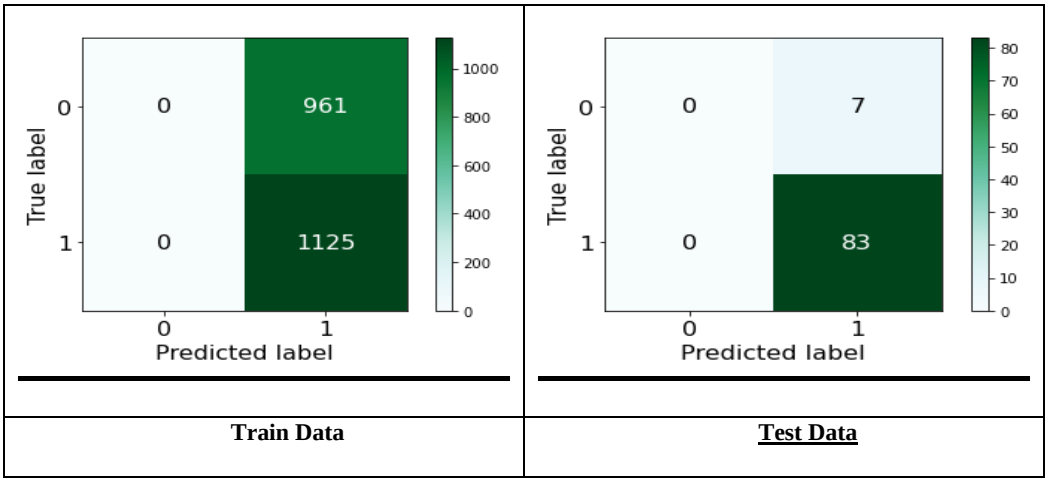

Train Data | **Test Data**

Fig 4-31: Confusion matrix after selecting softmax as activation function in dense layer

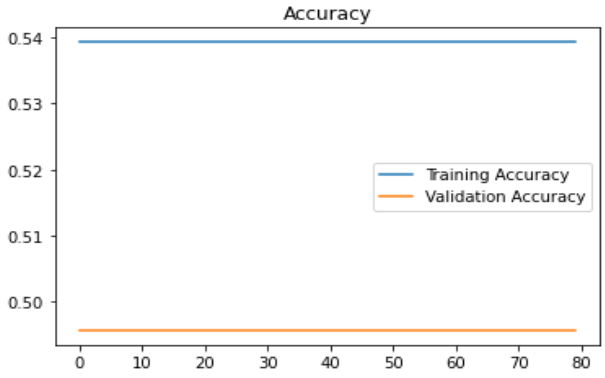

Fig 4-32: Train vs Validation Accuracy for each Epoch after selecting softmax activation function in dense layer

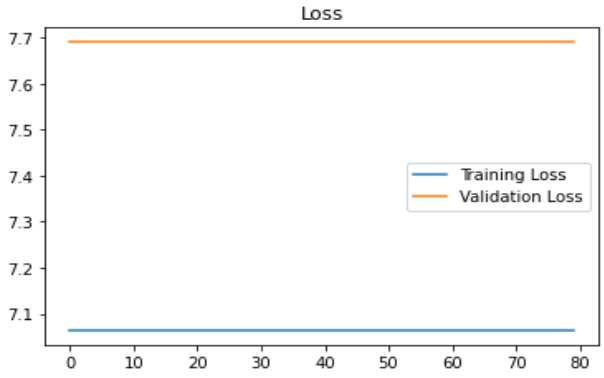

Fig 4-33: Train vs Validation Loss for each Epoch after selecting softmax activation function in dense layer

ReLU as Activation Function in Second Layer

Model	Accuracy (train)	Precision (train)	Recall (train)	F1_score (train)	Specificity (train)	Accuracy (test)	Precision (test)	Recall (test)	F1_score (test)	Specificity (test)
CNN	1.000	1.000	1.000	1.000	1.000	0.944	0.957	0.944	0.949	0.600

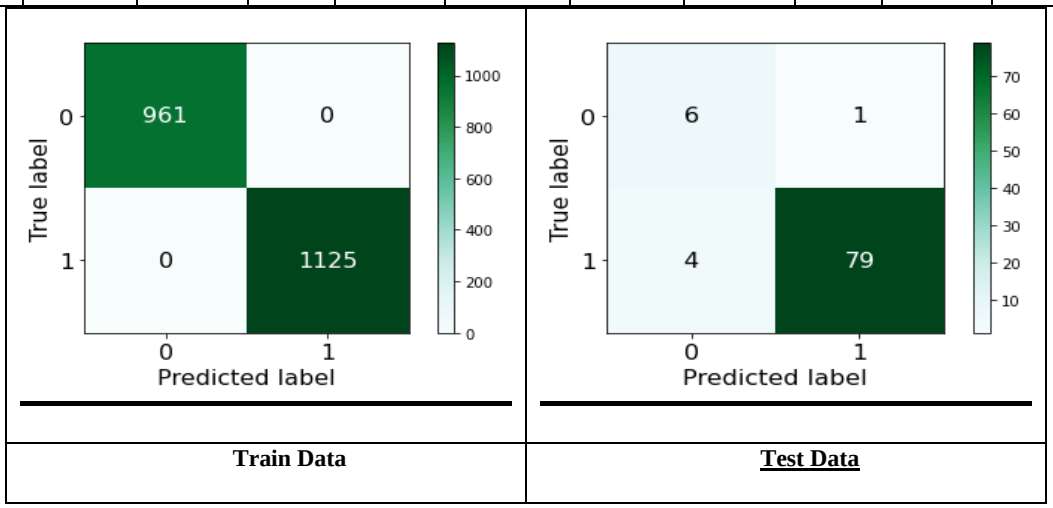

Train Data | **Test Data**

Fig 4-34: Confusion matrix after ReLU as activation function in second layer

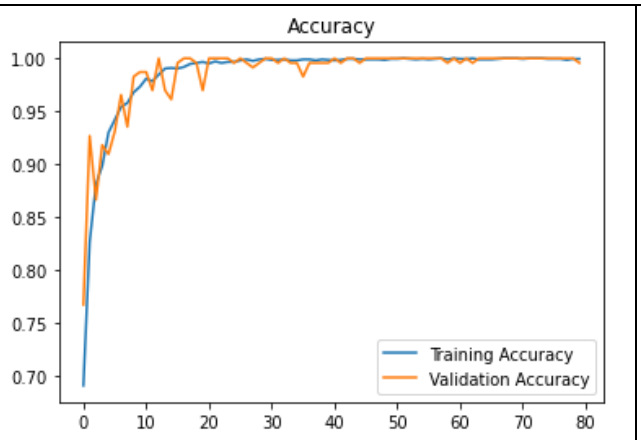

Fig 4-35: Train vs Validation Accuracy for each Epoch after ReLU as activation function in second layer

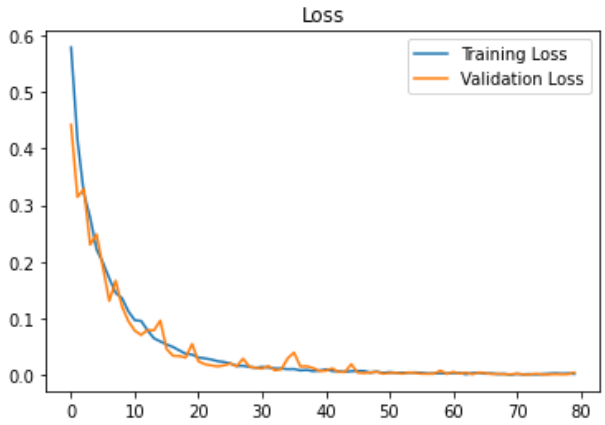

Fig 4-36: Train vs Validation Loss for each Epoch after ReLU as activation function in second layer

4.2.3 Selection of Pool Size

2x2 Maxpooling

Model	Accuracy (train)	Precision (train)	Recall (train)	F1_score (train)	Specificity (train)	Accuracy (test)	Precision (test)	Recall (test)	F1_score (test)	Specificity (test)
CNN	1.000	1.000	1.000	1.000	1.000	0.978	0.978	0.978	0.978	0.857

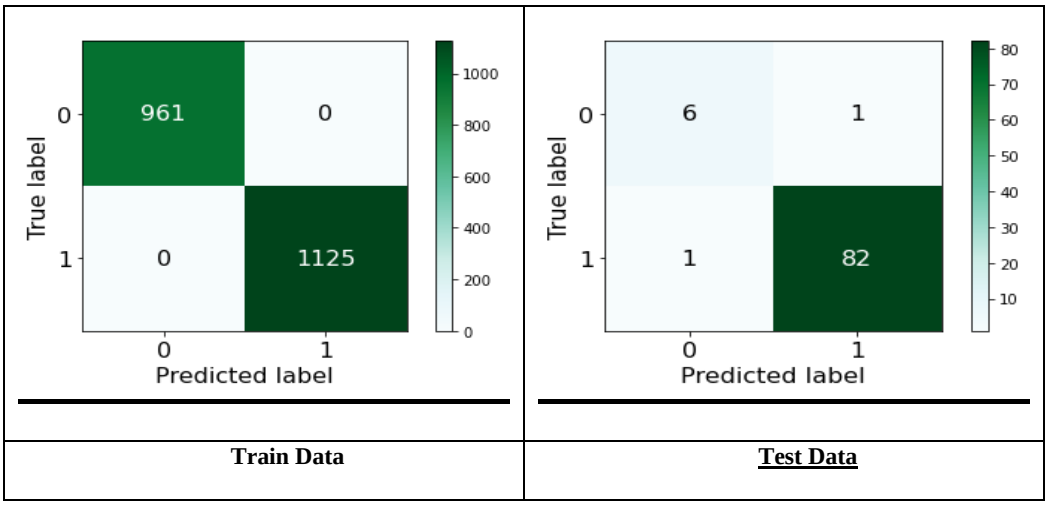

Train Data | **Test Data**

Fig 4-37: Confusion matrix after 2x2 maxpooling

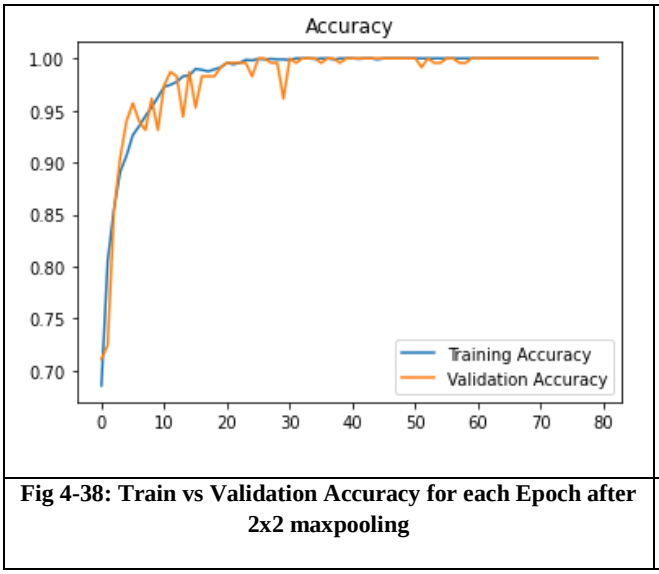

Fig 4-38: Train vs Validation Accuracy for each Epoch after 2x2 maxpooling

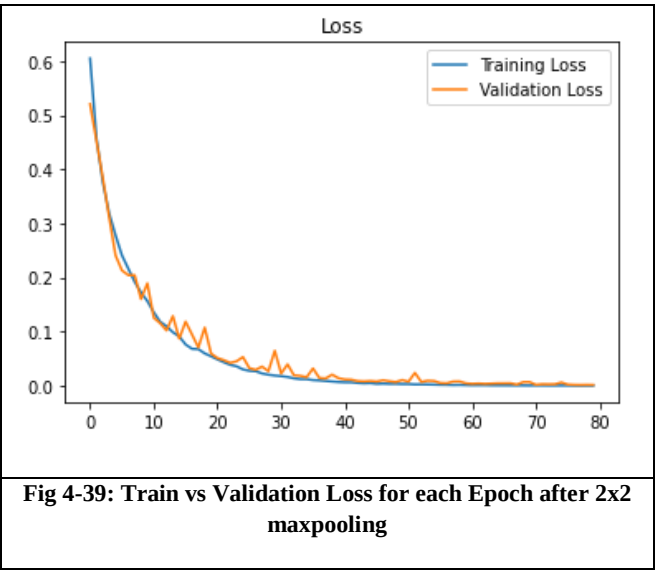

Fig 4-39: Train vs Validation Loss for each Epoch after 2x2 maxpooling

4.2.4 Performance of Classifiers

Different classifiers were applied on to the same dataset and hence, experiment results are obtained. While evaluating the performance of classifiers, default settings were used.

Support Vector Machine (SVM)

The parameters for training SVM model are as follows:

I. **Cost Function Value (C) :**
float, default value=1.0
Regularization parameter. The strength of the regularization is inversely proportional to C. Must be strictly positive. The penalty is a squared l2 penalty.

II. **Kernel:**
Options available:{'linear', 'poly', 'rbf', 'sigmoid', 'precomputed'}, default value='rbf'
Specifies the kernel type to be used in the algorithm

III. **Degree:**
int, default value=3
Degree of the polynomial kernel function ('poly'). Ignored by all other kernels.

IV. **Gamma:**
Options available {'scale', 'auto'} or float, default value='scale'
Kernel coefficient for 'rbf', 'poly' and 'sigmoid'.

V. **Coef:**
float, default value=0.0
Independent term in kernel function. It is only significant in 'poly' and 'sigmoid'.

VI. **Shrinking:**
bool, default value=True
Whether to use the shrinking heuristic.

VII. **Probability:**
bool, default value=False
It defines whether to enable probability estimates.

VIII. **cache_size:**
float, default value=200
Specify the size of the kernel cache (in MB).

IX. **Verbose:**
bool, default value=False
Enable verbose output. This setting takes advantage of a per-process runtime setting in libsvm that, if enabled, may not work properly in a multithreaded context.

X. **max_iter:**
int, default value=-1
Hard limit on iterations within solver, or -1 for no limit.

XI. **random_state:**
int, RandomState instance or None, default value=None
Controls the pseudo random number generation for shuffling the data for probability estimates

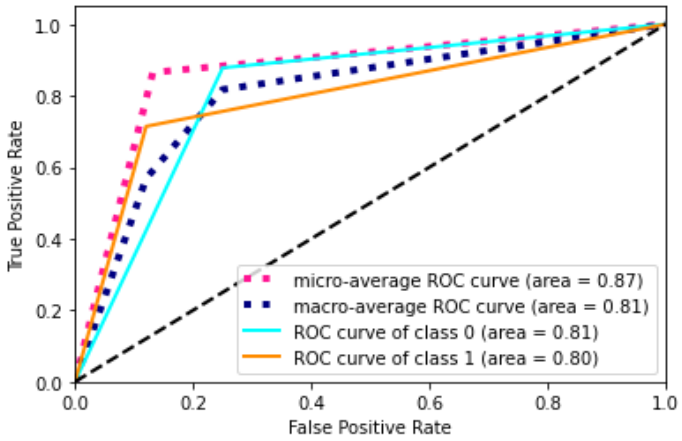

Fig 4-40: Receiver Operating Characteristic (ROC) Curve for SVM

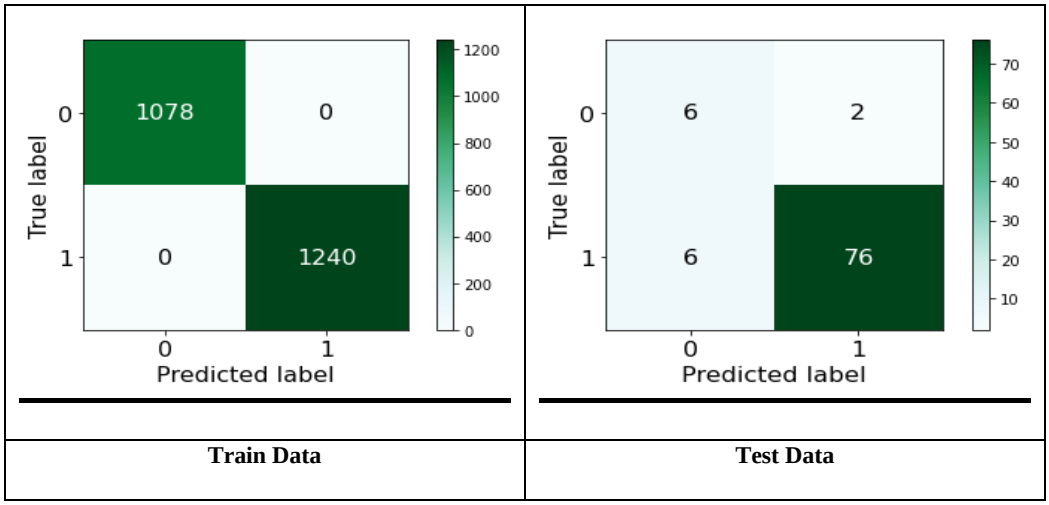

Train Data | **Test Data**

Fig 4-41: Confusion Matrix for SVM

Random Forest (RF)

The parameters for training RF model are as follows:

I. **n_estimators:** ***int, default value=100***
The number of trees in the forest.

II. **Criterion:**
Options available:*{"gini", "entropy"}, default value="gini"*
The function to measure the quality of a split. Supported criteria are "gini" for the Gini impurity and "entropy" for the information gain. : this parameter is tree-specific.

III. **max_depth:**
take *int variable, default value=None*
The maximum depth of the tree. If None, then nodes are expanded until all leaves are pure or until all leaves contain less than min_samples_split samples.

IV. **min_samples_split:**
take int or float variable, default value=2
The minimum number of samples required to split an internal node

V. **min_samples_leaf:**
take *int or float variable, default value=1*

The minimum number of samples required to be at a leaf node.

VI. **min_weight_fraction_leaf:**
float, default value=0.0
The minimum weighted fraction of the sum total of weights (of all the input samples) required to be at a leaf node.

VII. **max_features:**
Options available: {"auto", "sqrt", "log2"}, int or float, default value="auto"

The number of features to consider when looking for the best split:

- If int, then consider max_features features at each split.
- If float, then max_features is a fraction and round(max_features * n_features) features are considered at each split.
- If "auto", then max_features=sqrt(n_features).
- If "sqrt", then max_features=sqrt(n_features) (same as "auto").
- If "log2", then max_features=log2(n_features).

• If None, then max_features=n_features.

VIII. max_leaf_nodes:

take *int variable, default value=None*

Grow trees with max leaf nodes in best-first fashion. Best nodes are defined as relative reduction in impurity. If None then unlimited number of leaf nodes.

IX. min_impurity_decrease:

take *float variable, default value=0.0*

A node will be split if this split induces a decrease of the impurity greater than or equal to this value.

X. min_impurity_split:

take *float variable, default value=None*

Threshold for early stopping in tree growth. A node will split if its impurity is above the threshold, otherwise it is a leaf.

XI. Bootstrap:

take *bool variable, default value=True*

Whether bootstrap samples are used when building trees. If False, the whole dataset is used to build each tree.

XII. oob_score:

take *bool variable, default value=False*

Whether to use out-of-bag samples to estimate the generalization accuracy.

XIII. n_jobs:

int, default value=None

The number of jobs to run in parallel.

XIV. random_state:

int, RandomState instance or None, default value=None

Controls both the randomness of the bootstrapping of the samples used when building

XV. Verbose:

int, default value=0

Controls the verbosity when fitting and predicting.

XVI. warm_start:

bool, default value=False

When set to True, reuse the solution of the previous call to fit and add more estimators to the ensemble, otherwise, just fit a whole new forest.

XVII. class_weight*{"balanced", "balanced_subsample"}, dict or list of dicts, default value=None*

Weights associated with classes in the form {class_label: weight}. If not given, all classes are supposed to have weight one. For multi-output problems, a list of dicts can be provided in the same order as the columns of y.

XVIII. ccp_alpha:

non-negative float, default value=0.0

Complexity parameter used for Minimal Cost-Complexity Pruning. The subtree with the largest cost complexity that is smaller than `ccp_alpha` will be chosen. By default value, no pruning is performed.

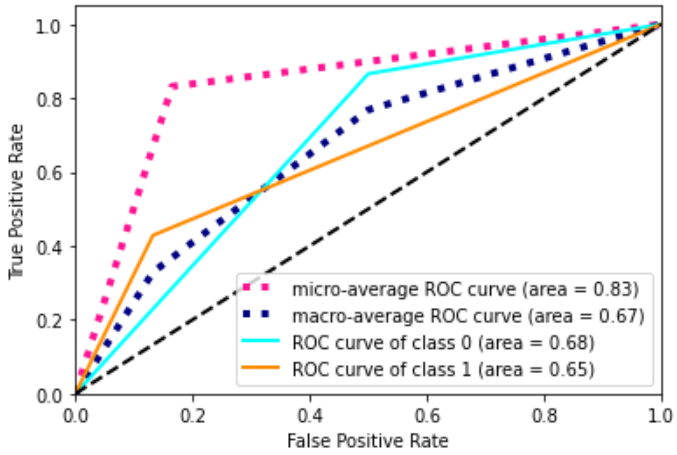

Fig 4-42: Receiver Operating Characteristic (ROC) Curve for RF

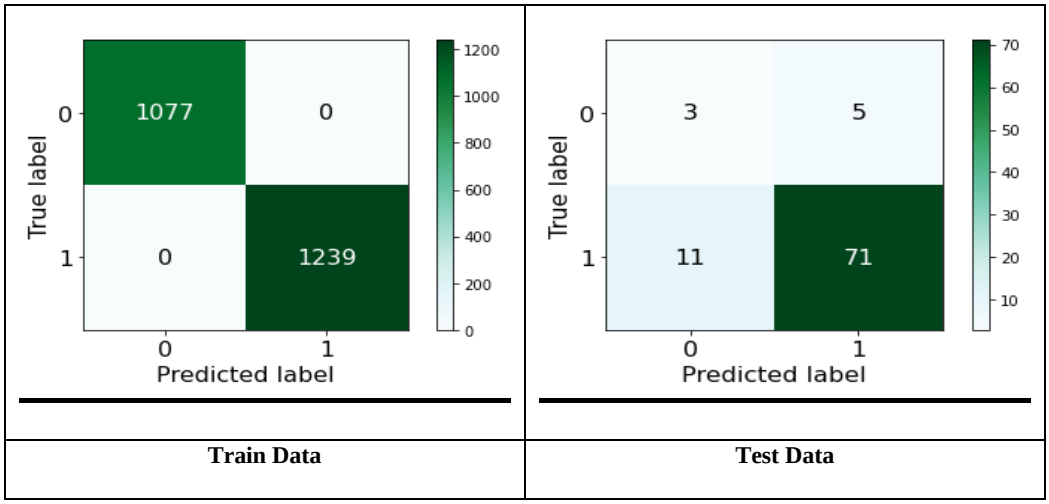

Train Data | **Test Data**

Fig 4-43: Confusion Matrix for RF

Decision Tree (DT)

The parameters for training DT model are as follows:

I. **Criterion:**
Options available: {"gini", "entropy"}, default value="gini"
The function to measure the quality of a split. Supported criteria are "gini" for the Gini impurity and "entropy" for the information gain.

II. **Splitter:**
Options available: {"best", "random"}, default value="best"
The strategy used to choose the split at each node. Supported strategies are "best" to choose the best split and "random" to choose the best random split.

III. **max_depth:**
take int variable, default value=None
The maximum depth of the tree. If None, then nodes are expanded until all leaves are pure or until all leaves contain less than min_samples_split samples.

IV. **min_samples_split:**
take *int or float variable, default value=2*
The minimum number of samples required to split an internal node

V. **min_samples_leaf:**
take *int or float variable , default value=1*

The minimum number of samples required to be at a leaf node.

VI. **min_weight_fraction_leaf:** ***float, default value=0.0***
The minimum weighted fraction of the sum total of weights (of all the input samples) required to be at a leaf node.

VII. **max_features**
take int, float or {"auto", "sqrt", "log2"}, default value=None
The number of features to consider when looking for the best split

VIII. **random_state:**
take *int, RandomState instance or None, default value=None*
Controls the randomness of the estimator.

IX. **max_leaf_nodes:**
take *int variable, default value=None*
Grow a tree with max leaf node in best-first fashion. Best nodes are defined as relative reduction in impurity. If None then unlimited number of leaf nodes.

X. **min_impurity_decrease:**
take *float variable, default value=0.0*
A node will be split if this split induces a decrease of the impurity greater than or equal to this value.

XI. min_impurity_split:

take *float variable, default value=0*

Threshold for early stopping in tree growth. A node will split if its impurity is above the threshold, otherwise it is a leaf.

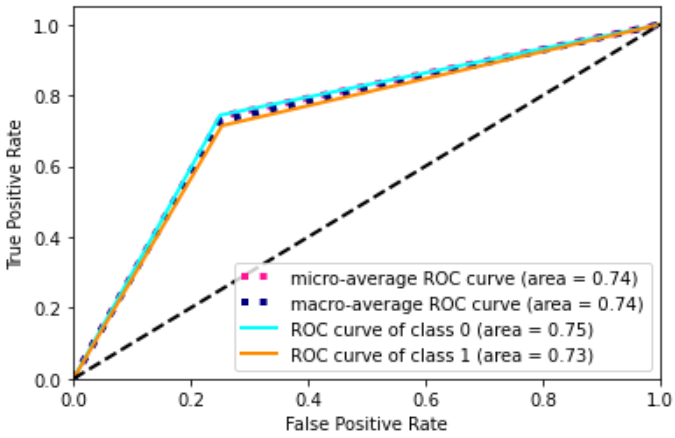

Fig 4-44: Receiver Operating Characteristic (ROC) Curve for DT

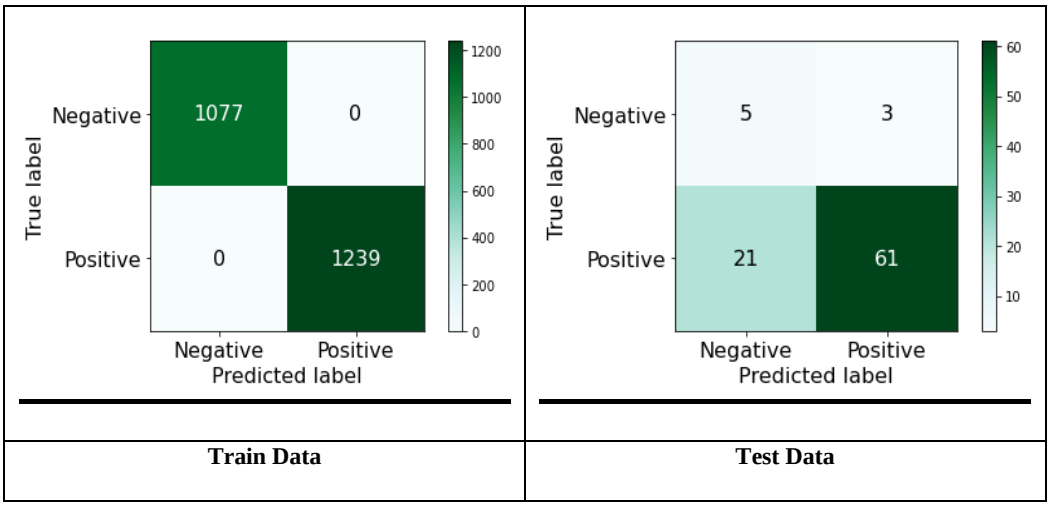

Train Data	Test Data

Fig 4-45: Confusion Matrix for DT

K Nearest Neighbor (KNN):

The parameters for training KNN model are as follows:

I. **n_neighbors:**
int, default value=5
Number of neighbors to use by default value for **kneighbors** queries.

II. **Weights:**
Options available: ***{'uniform', 'distance'} or callable, default value='uniform'***
weight function used in prediction. Possible values:

- uniform' : uniform weights. All points in each neighborhood are weighted equally.
- 'distance' : weight points by the inverse of their distance. in this case, closer neighbors of a query point will have a greater influence than neighbors which are further away.
- [callable] : a user-defined function which accepts an array of distances, and returns an array of the same shape containing the weights.

III. '**algorithm:**
Options available:{'auto', 'ball_tree', 'kd_tree', 'brute'}, default value='auto'
Algorithm used to compute the nearest neighbors:

- 'ball_tree' will use **BallTree**
- 'kd_tree' will use **KDTree**
- 'brute' will use a brute-force search.
- 'auto' will attempt to decide the most appropriate algorithm based on the values passed to **fit** method.

IV. **leaf_size:**
int, default value=30
Leaf size passed to BallTree or KDTree. This can affect the speed of the construction and query, as well as the memory required to store the tree. The optimal value depends on the nature of the problem.

V. **metric_params:**
dict variable, default value=None
Additional keyword arguments for the metric function.

VI. **n_jobs:** ***int, default value=None***
The number of parallel jobs to run for neighbors search.

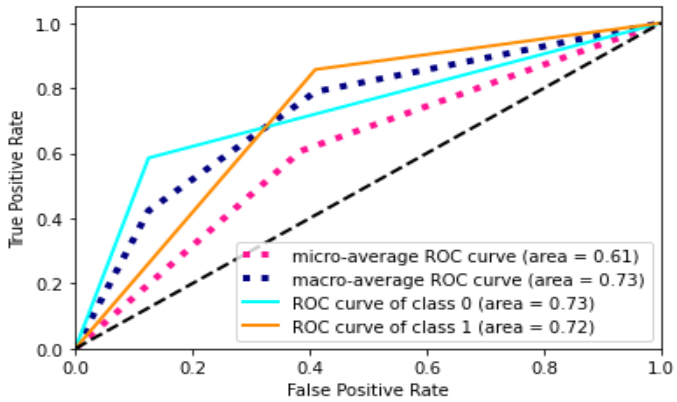

Fig 4-46: Receiver Operating Characteristic (ROC) Curve for KNN

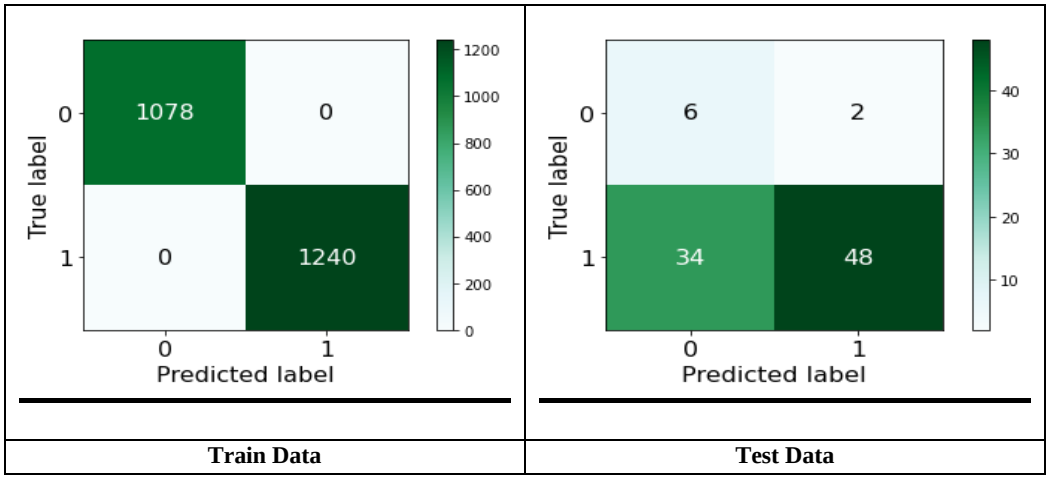

Train Data	Test Data

Fig 4-47: Confusion Matrix for KNN

Multilayer Perceptron (MLP)

The parameters for training MLP model are as follows:

I. **hidden_layer_sizes:**
tuple, length = n_layers - 2, default value=(100,)
The ith element represents the number of neurons in the ith hidden layer.

II. **Activation**
Options available: ***{'identity', 'logistic', 'tanh', 'relu'}, default value='relu'***
Activation function for the hidden layer.

- 'identity', no-op activation, useful to implement linear bottleneck, returns f(x) = x
- 'logistic', the logistic sigmoid function, returns f(x) = 1 / (1 + exp(-x)).
- 'tanh', the hyperbolic tan function, returns f(x) = tanh(x).
- 'relu', the rectified linear unit function, returns f(x) = max(0, x)

III. **Solver:**
Options available: {'lbfgs', 'sgd', 'adam'}, default value='adam'
The solver for weight optimization.

- 'lbfgs' is an optimizer in the family of quasi-Newton methods.
- 'sgd' refers to stochastic gradient descent.
- 'adam' refers to a stochastic gradient-based optimizer proposed
-

IV. **Alpha:**
float, default value=0.0001
L2 penalty (regularization term) parameter.

V. **batch_size*int, default value='auto'***
Size of minibatches for stochastic optimizers. If the solver is 'lbfgs', the classifier will not use minibatch.

VI. **learning_rate*{'constant', 'invscaling', 'adaptive'}, default value='constant'***
Learning rate schedule for weight updates.

- 'constant' is a constant learning rate given by 'learning_rate_init'.
- 'invscaling' gradually decreases the learning rate at each time step 't' using an inverse scaling exponent of 'power_t'. effective_learning_rate = learning_rate_init / pow(t, power_t)
- 'adaptive' keeps the learning rate constant to 'learning_rate_init' as long as training loss keeps decreasing. Each time two consecutive epochs fail to decrease training loss by at least tol, or fail to increase validation score by at least tol if 'early_stopping' is on, the current learning rate is divided by 5.

VII. **power_t:** ***double, default value=0.5***
The exponent for inverse scaling learning rate. It is used in updating effective learning rate when the learning_rate is set to 'invscaling'. Only used when solver='sgd'.

VIII. **max_iter:**
int, default value=200
Maximum number of iterations to use.

IX. **Shuffle:**
bool, default value=True
Whether to shuffle samples in each iteration. Only used when solver=’sgd’ or ‘adam’.

X. **random_state:**
int, RandomState instance, default value=None
Determines random number generation for weights and bias initialization, train-test split if early stopping is used, and batch sampling when solver=’sgd’ or ‘adam’. Pass an int for reproducible results across multiple function calls.

XI. **warm_start:**
bool, default value=False
When set to True, reuse the solution of the previous call to fit as initialization, otherwise, just erase the previous solution.

XII. **Momentum:**
float, default value=0.9
Momentum for gradient descent update. Should be between 0 and 1. Only used when solver=’sgd’.

XIII. **early_stopping:**
bool, default value=False
Whether to use early stopping to terminate training when validation score is not improving

XIV. **validation_fraction:**
float, default value=0.1
The proportion of training data to set aside as validation set for early stopping. Must be between 0 and 1. Only used if early_stopping is True

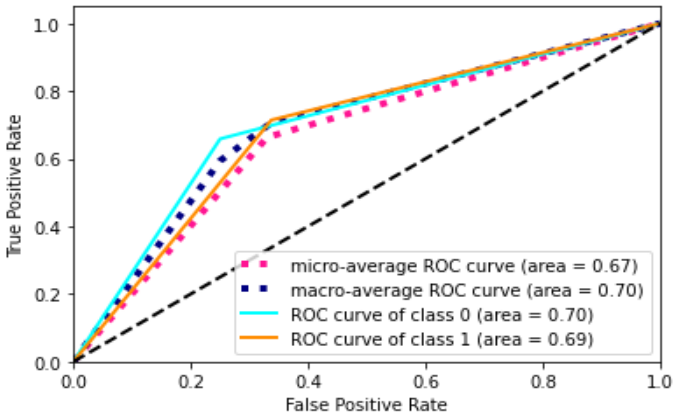

Fig 4-48: Receiver Operating Characteristic (ROC) Curve for MLP

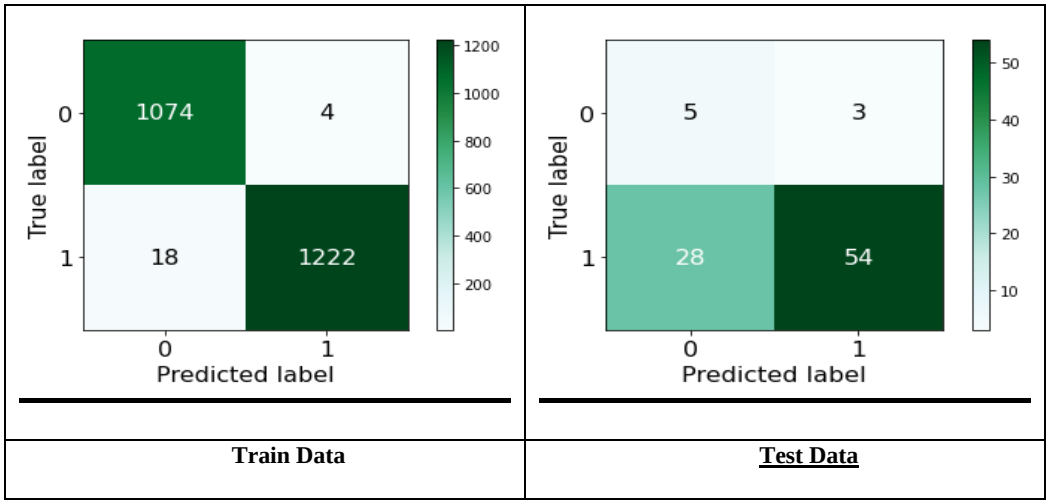

Train Data | **Test Data**

Fig 4-49: Confusion Matrix for MLP

Naïve Bayes (NB)

The parameters for training NB model are as follows:

I. **Priors:**
array-like of shape (n_classes,)
Prior probabilities of the classes. If specified the priors are not adjusted according to the data.

II. **var_smoothing:**
float, default value=1e-9
Portion of the largest variance of all features that is added to variances for calculation stability.

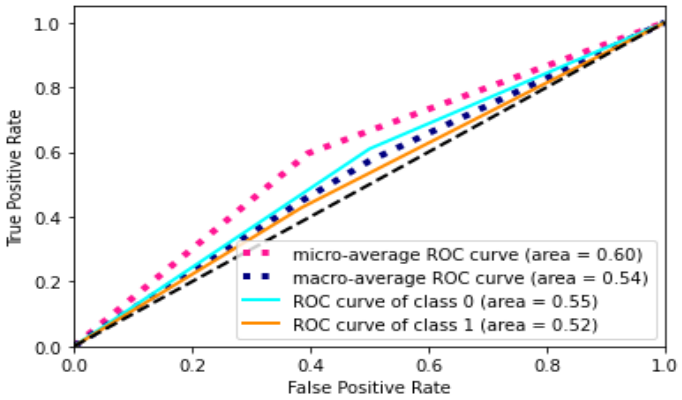

Fig 4-50: Receiver Operating Characteristic (ROC) Curve for NB

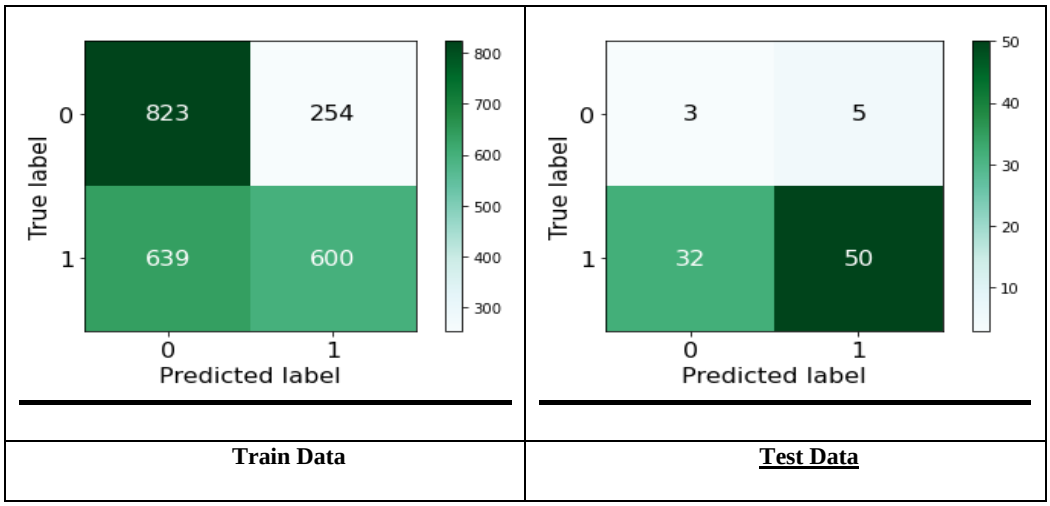

Train Data | **Test Data**

Fig 4-51: Confusion Matrix for NV

4.2.5 Summary

Now from the above figures as we can see that, the filter size 32 gives optimal result than other chosen filter sizes (16, 28, 40). The hyper parameters of the model were further tuned for activation function and also for max pooling. Different classifiers like Random Forest (RF), Support Vector Machine (SVM), Decision Tree (DT), K-Nearest Neighbor (KNN), Multilayer Perceptron (MLP), Naïve Bayes (NV) were applied on to the same dataset and experiment results are obtained. While evaluating the performance of classifiers, default settings were used. Finally, performance is summarized in the below table:

Model	Accuracy	Precision	Recall	F1 Score	Specificity
Random Forest	0.822	0.870	0.822	0.843	0.214
SVM	0.856	0.960	0.878	0.917	0.333
Decision Tree	0.549	0.81	0.472	0.596	0.367
KNN	0.600	0.888	0.600	0.685	0.150
MLP	0.656	0.877	0.656	0.730	0.152
Naive Bayes	0.589	0.836	0.589	0.677	0.086
CNN	0.978	0.988	0.988	0.988	0.857

Table 4-1: Performance of different models

From the above table, we can see that CNN outperformed all the other methods showing 97.8% accuracy.

CHAPTER 5

CONCLUSION

This chapter discusses the main outcomes and contribution of this thesis, followed by highlighting the thesis contribution, thesis limitations and future work.

5.1 Main Outcomes

As MRI-based medical image analysis for brain tumor studies has been gaining attention in recent times due to an increased need for efficient and objective evaluation of large amounts of medical data, in this thesis, two very effective techniques are proposed for the isolation of tumorous cells from MRI images. First approach used conventional machine learning where SVM was applied to validate the results. In the second approach, deep learning technique (CNN) was applied. The outcomes of the approaches are:

5.1.1 Research Activity One (Conventional ML)

MRI gray scale images are considered as test inputs which have been collected from pathological experts where 3 different batches were incorporated and these test images comprises different types of glioma, meningioma and pituitary tumor. The first move towards the solution was to enhance the images to minimize the issues with contrast. The gray scale images were converted to RGB images and then to HSV to obtain better result in terms of contrast. After carrying out local histogram equalization, the images were converted back to RGB images. For the first time, in this thesis, morphological operation is used as a filter operation to reduce unwanted regions. The last and indispensable step of pre-processing is to apply segmentation to split the images in regions into two classes-

foreground and background. Threshold based Otsu's method is chosen in this step for less computing time only on G and B were considered for segmentation.

The post-processing method includes two steps which are feature extraction and identification. Unwanted features must be excluded during feature extraction process to avoid erroneous identification. Features are categorized in three different regions- shape, size and color. As the images became binary after segmentation, color was not included as a candidate of feature extraction. This study incorporated pathology laboratory experts' used shape and size features which include regions area, circularity, solidity, roundness, radius, and diameter. Thus, this work only incorporates size and shape for feature extraction. Here, again morphological operation was used to identify the region of interests (ROI).

From the study, it is shown that this method gives 96.23% accuracy in average. According to pathology lab experts, **85%±7** accuracy rate is accepted, so in this case, this method obtaining 96.23% accuracy is very much acceptable by the pathology experts. To further increase the efficiency of the proposed framework, classification techniques such as SVM classification was applied to select the most discriminative features to help classify the structural elements. Unfortunately, the exactitude did not change after SVM classification. Thus, this is not included as a step for this approach.

5.1.2 Research Activity Two (Deep ML)

For this approach, Convolutional Neural Network is applied on the same set of data as the previous approach. In this approach, vgg16 pre-trained model is used for Large-Scale Image Recognition. After that, 2D Convolutional layer, Keras Conv2D is applied with filter size 32. In this thesis, we also tried to change the filter size (40, 32, 16) to get more

optimal result. Unfortunately, filer size other than 32 could not provide optimal results in Confusion Matrix (CM) also in Train vs Validation Accuracy for each Epoch which was shown in previous chapter. By selecting RELU as the activation function in the Dense Layer also did not perform as expected but Sigmoid showed optimal results. In the following stage, Max Pooling is used. Here, by selecting size 2x2 Max Pooling failed to perform optimally but after selecting size 4x4 for Max Pooling showed better results. Also, 50% drop out is used. Increment in percentage of drop out increased number of nodes in the layers whereas decrement in percentage of drop out increased computational intensity. In the dense layer, use of Softmax as activation function did not show optimal results whereas application of Sigmoid to predict the probability as an output as activation function showed optimal results. Providently, this approach gives 97.84% accuracy on average.

5.2 Thesis Contributions

As $\pm 17\%$ accuracy is accepted by pathology experts, both the approaches have proved success in this matter. However, there is slight trade-off between the approaches. The second proposed framework for deep machine learning approach giving 97.84% accuracy is computational intensive. Thus this approach needs a bit more time to process. On the other hand, the first one- conventional machine learning approach which gives a less accuracy (96.23%) than the second method requires less computing time. Thus, there is a trade-off between these two methods. The experts need to choose between these two depending on their demand. If they choose to have more accuracy that is 97.84% and have high-configured PC, they should go for the deep machine learning approach. And if anyone has any issue with time means want the result in less time or does not have high configured PCs in hand, must choose the first approach giving 96.23% accuracy which is

also very much acceptable by the experts as it is also a very good amount of accuracy. The above mentioned accuracy two important aspects:

a. It is observed that there is no Benchmark Dataset which can be used to compare existing approaches. In this study both the approaches used the same data which gives scope of comparing the approaches.

b. In the first approach (Conventional ML), morphological operation is used instead of usual filter operation for noise reduction. This also showed better accuracy level.

c. In the second approach (Deep ML), study is carried out on different setting which ultimately helped proposing a suitable framework.

d. In the same approach, parameter tuning was carried out involving an exhaustive study which ultimately helped for proposing a suitable framework.

e. There is a scope of data collaboration. The dataset made available for this study may be used as Benchmark Dataset (with prior permission from the originator).

5.3 Thesis Limitations

While carrying out the study, it was revealed that:

a. There is no Benchmark Dataset which can be used to compare existing approaches for detection of brain tumors from MRI images.

b. Huge volume of data was not available which actually a prerequisite for the second approach was (Deep ML).

5.4 Future Works

As MRI-based medical image analysis for brain tumor studies has been gaining attention in recent times due to an increased need for efficient approach, there is huge scope of further study in this sector. However, for the study carried out by this researcher, followings can be done:

a. A comparative study can be carried out for proposing the appropriate pre-trained model for the second approach (vgg16 used by this researcher).

b. A Benchmark Dataset may be contributed by appropriate Medical Authority for carrying out comparisons of the existing approaches.

c. Present work identifies tumor regions mainly from 2D data. The research may extend to identification process for 3D data as well.

d. Grading of tumors can be obtained if more volume of data is available (collaboration with hospitals may ensure the availability of huge volume of data).

e. Other approaches may be compared for performance with application of same set of data.

References

[1] S. C. Lester, *Manual of Surgical Pathology*. Elsevier Health Sciences, 2010.

[2] O. Sertel, U. V. Catalyurek, H. Shimada, and M. N. Gurcan, "Computer- aided prognosis of neuroblastoma: Detection of mitosis and karyorrhexis cells in digitized histological images," in *2009 Annual International Conference of the IEEE Engineering in Medicine and Biology Society*. IEEE, 2009, pp. 1433–1436.

[3] T. Kelsey, B. Caserta, L. Castillo, H. Wallace, and F. C. Gonzálvez, "Proliferating cell nuclear antigen (pcna) allows the automatic identi- fication of follicles in microscopic images of human ovarian tissue," *Nature Precedings*, pp. 1–1, 2010.

[4] T. H. Van der Kwast, A. Evans, G. Lockwood, D. Tkachuk, D. G. Bost- wick, J. I. Epstein, P. A. Humphrey, R. Montironi, G. J. Van Leenders, C.-G. Pihl *et al.*, "Variability in diagnostic opinion among pathologists for single small atypical foci in prostate biopsies," *The American journal of surgical pathology*, vol. 34, no. 2, pp. 169–177, 2010.

[5] S. Kothari, J. H. Phan, T. H. Stokes, and M. D. Wang, "Pathology imaging informatics for quantitative analysis of whole-slide images," *Journal of the American Medical Informatics Association*, vol. 20, no. 6, pp. 1099–1108, 2013.

[6] M. R. Lamprecht, D. M. Sabatini, and A. E. Carpenter, "Cellpro- filer™: free, versatile software for automated biological image analysis," *Biotechniques*, vol. 42, no. 1, pp. 71–75, 2007.

[7] V. Kiruthika and M. Ramya, "Automatic segmentation of ovarian follicle using k-means clustering," in *2014 fifth international conference on signal and image processing*. IEEE, January 8-10, 2014, pp. 137–141.

[8] A. Skodras, S. Giannarou, M. Fenwick, S. Franks, J. Stark, and K. Hardy, "Object recognition in the ovary: quantification of oocytes from micro- scopic images," in *2009 16th International Conference on Digital Signal Processing*. IEEE, 2009, pp. 1–6.

[9] S. A. Nishu, "Quantifying the defect visibility in digital images by proper color space selection," *International journal of engineering research and applications*, vol. 2, no. 3, pp. 1764–1767, 2012.

[10] A. Entwistle, "Moderated histogram equalization, an automatic means of enhancing the contrast in digital light micrographs reversibly," *Journal of microscopy*, vol. 214, no. 3, pp. 272–286, 2004.

[11] A. Entwistle “A method for the blind correction of the effects of attenuation and shading in light micrographs based upon moderated histogram equalization,” *Journal of microscopy*, vol. 219, no. 3, pp. 141–156, 2005.

[12] K. Bapure, “Automated image analysis for nuclear morphometry using h&e and feulgen stains in prostate biopsies,” Ph.D. dissertation, Univer- sity of Illinois at Chicago, 2012.

[13] X. Liu, J. Tan, I. Hatem, and B. L. Smith, “Image processing of hema- toxylin and eosin-stained tissues for pathological evaluation,” *Toxicology mechanisms and methods*, vol. 14, no. 5, pp. 301–307, 2004.

[14] P. Kaur, G. Singh, and P. Kaur, “Classification and validation of mri brain tumor using optimised machine learning approach,” in *ICDSMLA 2019*. Springer, 2020, pp. 172–189.

[15] C. A. Picut, C. L. Swanson, K. L. Scully, V. C. Roseman, R. F. Parker, and A. K. Remick, “Ovarian follicle counts using proliferating cell nuclear antigen (pcna) and semi-automated image analysis in rats,” *Toxicologic pathology*, vol. 36, no. 5, pp. 674–679, 2008.

[16] G. Landini and I. Othman, “Estimation of tissue layer level by sequential morphological reconstruction,” *Journal of microscopy*, vol. 209, no. 2, pp. 118–125, 2003.

[17] D. G. Rosen, X. Huang, M. T. Deavers, A. Malpica, E. G. Silva, and J. Liu, “Validation of tissue microarray technology in ovarian carcinoma,” *Modern pathology*, vol. 17, no. 7, pp. 790–797, 2004.

[18] T. Y. Goh, S. N. Basah, H. Yazid, M. J. A. Safar, and F. S. A. Saad, “Performance analysis of image thresholding: Otsu technique,” *Measurement*, vol. 114, pp. 298–307, 2018.

[19] S. R. Telrandhe, A. Pimpalkar, and A. Kendhe, “Detection of brain tumor from mri images by using segmentation & svm,” in *2016 World Conference on Futuristic Trends in Research and Innovation for Social Welfare (Startup Conclave)*. IEEE, 2016, pp. 1–6.

[20] R. Ahmmed and M. F. Hossain, “Tumor detection in brain mri image using template based k-means and fuzzy c-means clustering algorithm,” in *2016 International Conference on Computer Communication and Informatics (ICCCI)*. IEEE, 2016, pp. 1–6.

[21] M.-N. Wu, C.-C. Lin, and C.-C. Chang, “Brain tumor detection using color-based k-means clustering segmentation,” in *Third International Conference on Intelligent Information Hiding and Multimedia Signal Processing (IIH-MSP 2007)*, vol. 2. IEEE, 2007, pp. 245–250.

[22] M. M. Thaha, K. P. M. Kumar, B. Murugan, S. Dhanasekeran, P. Vijayakarthick, and A. S. Selvi, "Brain tumor segmentation using convo- lutional neural networks in mri images," *Journal of medical systems*, vol. 43, no. 9, pp. 1–10, 2019.

[23] S. T. Kebir and S. Mekaoui, "An efficient methodology of brain abnormalities detection using cnn deep learning network," in *2018 International Conference on Applied Smart Systems (ICASS)*. IEEE, 2018, pp. 1–5.

[24] R. Vinoth and C. Venkatesh, "Segmentation and detection of tumor in mri images using cnn and svm classification," in *2018 Conference on Emerging Devices and Smart Systems (ICEDSS)*. IEEE, 2018, pp. 21– 25.

[25] M. Ben naceur , R. Saouli, M. Akil, R. Kachouri *et al.*, "Fully automatic brain tumor segmentation using end-to-end incremental deep neural networks in mri images," *Computer methods and programs in biomedicine*, vol. 166, pp. 39–49, 2018.

[26] H. Mohsen, E.-S. A. El-Dahshan, E.-S. M. El-Horbaty, and A.-B. M. Salem, "Classification using deep learning neural networks for brain tumors," *Future Computing and Informatics Journal*, vol. 3, no. 1, pp. 68–71, 2018.

[27] M. Havaei, A. Davy, D. Warde-Farley, A. Biard, A. Courville, Y. Bengio, C. Pal, P.-M. Jodoin, and H. Larochelle, "Brain tumor segmentation with deep neural networks," *Medical image analysis*, vol. 35, pp. 18–31, 2017.

[28] S. Damodharan and D. Raghavan, "Combining tissue segmentation and neural network for brain tumor detection." *International Arab Journal of Information Technology (IAJIT)*, vol. 12, no. 1, 2015.

[29] T. Pandiselvi and R. Maheswaran, "Efficient framework for identifying, locating, detecting and classifying mri brain tumor in mri images," *Journal of medical systems*, vol. 43, no. 7, pp. 1–14, 2019.

[30] A. Tiwari, S. Srivastava, and M. Pant, "Brain tumor segmentation and classification from magnetic resonance images: Review of selected methods from 2014 to 2019," *Pattern Recognition Letters*, vol. 131, pp. 244–260, 2020.

[31] I. Wahlang, P. Sharma, S. M. Nasreen, A. K. Maji, and G. Saha, "A comparative study on segmentation techniques for brain tumor mri," in *Information and Communication Technology for Competitive Strategies*. Springer, 2019, pp. 665–673.

[32] A. A. TEGEGNE, "Brain tumor detection based on magnetic resonance image analysis", M.Sc thesis, Biomedical Engineering, Addis Ababa Univ., Ethiopia, 2018. Accessed on: 21 March, 2020. [Online]. Available:

http://etd.aau.edu.et/bitstream/handle/123456789/15546/Amare%20Ambaw.pdf?sequence=1&isAllowed=y

[33] T. Logeswari and M. Karnan, "An improved implementation of brain tumor detection using segmentation based on soft computing," *Journal of Cancer Research and Experimental Oncology*, vol. 2, no. 1, pp. 006– 014, 2009.

[34] M. M. Chanu and K. Thongam, "Computer-aided detection of brain tumor from magnetic resonance images using deep learning network," *Journal of Ambient Intelligence and Humanized Computing*, pp. 1–12, 2020.

[35] K. H. Shibly, S. K. Dey, M. T.-U. Islam, and M. M. Rahman, "Covid faster r–cnn: A novel framework to diagnose novel coronavirus disease (covid-19) in x-ray images," *Informatics in Medicine Unlocked*, vol. 20, p. 100405, 2020.

[36] N. Kumari and S. Saxena, "Review of brain tumor segmentation and classification," in *2018 International Conference on Current Trends towards Converging Technologies (ICCTCT)*. IEEE, 2018, pp. 1–6.

[37] J. Wainer, "Comparison of 14 different families of classification algo- rithms on 115 binary datasets," *arXiv preprint arXiv:1606.00930*, 2016.

[38] T. S. Sazzad, L. Armstrong, and A. K. Tripathy, "An automated detection process to detect ovarian tissues using type p63 digitized color images," in *2015 IEEE 27th International Conference on Tools with Artificial Intelligence (ICTAI)*. IEEE, 2015, pp. 278–285.

[39] E. Block, "Quantitative morphological investigations of the follicular system in women," *Cells Tissues Organs*, vol. 14, no. 1-2, pp. 108–123, 1952.

[40] B. Bolon, T.J. Bucci, A.R. Warbritton, J.J. Chen, D.R. Mattison and J.J. Hemdel, "Differential follicle counts as a screen for chemically induced ovarian toxicity in mice: results from continuous breeding bioassays," *Fundamental and applied toxicology*, vol. 39, no. 1, pp. 1– 10, 1997.

[41] T. J. Bucci, B. Bolon, A. R. Warbritton, J. J. Chen, and J. J. Heindel, "Influence of sampling on the reproducibility of ovarian follicle counts in mouse toxicity studies," *Reproductive Toxicology*, vol. 11, no. 5, pp. 689–696, 1997.

[42] S. Geber, R. Megale, F. Vale, A. M. A. Lanna, and A. C. V. Cabral, "Variation in ovarian follicle density during human fetal development," *Journal of assisted reproduction and genetics*, vol. 29, no. 9, pp. 969– 972, 2012.

[43] M. N. Gurcan, L. E. Boucheron, A. Can, A. Madabhushi, N. M. Rajpoot, and B. Yener, "Histopathological image analysis: A review," *IEEE reviews in biomedical engineering*, vol. 2, pp. 147–171, 2009.

[44] E. Kaczmarek, A. Gorna, and P. Majewski, "Techniques of image anal- ysis for quantitative immunohistochemistry," *Rocz Akad Med Bialymst*, vol. 49, no. Suppl

1, pp. 155–158, 2004.
[45] U. Larsen and J. Menken, "Measuring sterility from incomplete birth histories," *Demography*, vol. 26, no. 2, pp. 185–201, 1989.
[46] J. Matthews, D. G. Altman, M. Campbell, and P. Royston, "Analysis of serial measurements in medical research." *British Medical Journal*, vol. 300, no. 6719, pp. 230–235, 1990.

[47] J. Menken, "Age and fertility: How late can you wait?" *Demography*, pp. 469–483, 1985.

[48] J. Menken and U. Larsen, "Fertility rates and aging," in *Aging, reproduction, and the climacteric*. Springer, 1986, pp. 147–166.

[49] J. Menken, J. Trussell, and U. Larsen, "Age and infertility," *Science*, vol. 233, no. 4771, pp. 1389–1394, 1986.

[50] A. S. Merseburger, M. A. Kuczyk, J. Serth, C. Bokemeyer, D. Y. Young, L. Sun, R. R. Connelly, D. G. McLeod, F. K. Mostofi, S. K. Srivastava *et al.*, "Limitations of tissue microarrays in the evaluation of focal alterations of bcl-2 and p53 in whole mount derived prostate tissues," *Oncology reports*, vol. 10, no. 1, pp. 223–228, 2003.

[51] P. B. Miller, J. S. Charleston, D. E. Battaglia, N. A. Klein, and M. R. Soules, "An accurate, simple method for unbiased determination of pri- mordial follicle number in the primate ovary," *Biology of reproduction*, vol. 56, no. 4, pp. 909–915, 1997.

[52] T. Mouroutis, S. J. Roberts, and A. A. Bharath, "Robust cell nuclei segmentation using statistical modelling," *Bioimaging*, vol. 6, no. 2, pp. 79–91, 1998.

[53] L. Muskhelishvili, S. K. Wingard, and J. R. Latendresse, "Proliferating cell nuclear antigen—a marker for ovarian follicle counts," *Toxicologic pathology*, vol. 33, no. 3, pp. 365–368, 2005.

[54] T. ShahriarSazzad, L. Armstrong, and A. Tripathy, "An automated approach to detect human ovarian tissues using type p63 counter stained histopathology digitized color images," in *2016 IEEE-EMBS International Conference on Biomedical and Health Informatics (BHI)*. IEEE, 2016, pp. 25–28.

[55] T. S. Sazzad, L. Armstrong, and A. K. Tripathy, "An automated ovarian tissue detection approach using type p63 non-counter stained images to minimize pathology experts observation variability," in *2016 IEEE EMBS Conference on Biomedical Engineering and Sciences (IECBES)*. IEEE, 2016, pp. 155–159.

[56] T. Sazzad, L. Armstrong, and A. K. Tripathy, "A comparative study of computerized approaches for type p63 ovarian tissues using histopathol- ogy digitized color images," 2016.

[57] T. S. Sazzad, L. Armstrong, and A. K. Tripathy, "A comprehensive analysis and review: Automated ovarian tissue detection using type p63 pathology color images," in *2016 13th International Joint Conference on Computer Science and Software*

Engineering (JCSSE). IEEE, 2016, pp. 1–6.

[58] T. S. Sazzad, L. Armstrong, and A. Tripathy, "A comprehensive analysis: Automated ovarian tissue detection using type p63 pathology color images," in *International Conference on Machine Learning and Data Mining in Pattern Recognition*. Springer, 2016, pp. 714–727.

[59] T. S. Sazzad, L. Armstrong, and A. K. Tripathy, "Type p63 digitized color images performs better identification for ovarian reproductive tissue analysis," in *2016 International Image Processing, Applications and Systems (IPAS)*. IEEE, 2016, pp. 1–6.

[60] T. S. Sazzad, L. Armstrong, and A. Tripathy, "Type p63 digitized color images performs better identification for ovarian tissue analysis." *Trans. Mass-Data Analysis of Images and Signals*, vol. 7, no. 1, pp. 41–51, 2016.

[61] T. S. Sazzad, L. Armstrong, and A. K. Tripathy, "Type p63 digitized color images performs better identification than other stains for ovarian tissue analysis," in *International Conference on Articulated Motion and Deformable Objects*. Springer, 2016, pp. 44–54.

[62] T. S. Sazzad, L. J. Armstrong, and A. K. Tripathy, "Type p63 non- counter stained digitized color images performs better identification than other stains for ovarian tissue analysis," in *2016 20th International Conference Information Visualisation (IV)*. IEEE, 2016, pp. 361–366.

[63] A. G. Smith, J. R. Howard, R. Kroll, P. Ramachandran, P. Hauer, J. R. Singleton, and J. McArthur, "The reliability of skin biopsy with measurement of intraepidermal nerve fiber density," *Journal of the neurological sciences*, vol. 228, no. 1, pp. 65–69, 2005.

[64] P. Souček and I. Gut, "Cytochromes p-450 in rats: structures, functions, properties and relevant human forms," *Xenobiotica*, vol. 22, no. 1, pp. 83–103, 1992.

[65] O. Tan and J. Fleming, "Proliferating cell nuclear antigen immunoreac- tivity in the ovarian surface epithelium of mice of varying ages and total lifetime ovulation number following ovulation," *Biology of reproduction*, vol. 71, no. 5, pp. 1501–1507, 2004.

[66] M. Teneriello, M. Ebina, R. Linnoila, M. Henry, J. Nash, R. Park, and M. Birrer, "p53 and ki-ras gene mutations in epithelial ovarian neoplasms," *Cancer research*, vol. 53, no. 13, pp. 3103–3108, 1993.

[67] M. Yoshida, A. Sanbuissyo, S. Hisada, M. Takahashi, Y. Ohno, and A. Nishikawa, "Morphological characterization of the ovary under normal cycling in rats and its viewpoints of ovarian toxicity detection," *The Journal of toxicological sciences*, vol. 34, no. Special, pp. SP189– SP197, 2009.